การตรวจสอบปริมาณรังสีทีจุดอ้างอิงในเทคนิค 3D และ IMRT โดยใช้โปรแกรมอิสระ

นายวิน เกา หวง

วิทยานิพนธ์นี้เป็นส่วนหนึ่งของการศึกษาตามหลักสูตรปริญญาวิทยาศาสตรมหาบัณฑิต
สาขาวิชาฉายาเวชศาสตร์ ภาควิชารังสีวิทยา
คณะแพทยศาสตร์ จุฬาลงกรณ์มหาวิทยาลัย
ปีการศึกษา 2556

REFERENCE POINT DOSE VERIFICATION IN 3D AND IMRT PLAN USING INDEPENDENT SOFTWARE

Mr. Vinh Cao Huu

A Thesis Submitted in Partial Fulfillment of the Requirements
for the Degree of Master of Science Program in Medical Imaging
Department of Radiology
Faculty of Medicine
Chulalongkorn University
Academic Year 2013

Thesis Title	REFERENCE POINT DOSE VERIFICATION IN 3D AND IMRT PLAN USING INDEPENDENT SOFTWARE
By	Mr. Vinh Cao Huu
Field of Study	Medical Imaging
Thesis Advisor	Associate Professor Sivalee Suriyapee, M.Eng.
Thesis Co-Advisor	Mr. Taweap Sanghangthum, Ph.D.

Accepted by the Faculty of Medicine, Chulalongkorn University in Partial Fulfillment of the Requirements for the Master's Degree

.....Dean of the Faculty of Medicine

(Associate Professor Sophon Napathorn, M.D.)

THESIS COMMITTEE

.....Chairman

(Associate Professor Kanjana Shotelersak, M.D.)

.....Thesis Advisor

(Associate Professor Sivalee Suriyapee, M.Eng.)

.....Thesis Co-Advisor

(Mr. Taweap Sanghangthum, Ph.D.)

.....External Examiner

(Professor Franco Milano, Ph.D.)

วิน เกา หวง : การตรวจสอบปริมาณรังสีทีจุดอ้างอิงในเทคนิค 3D และ IMRT โดยใช้โปรแกรมอิสระ. (REFERENCE POINT DOSE VERIFICATION IN 3D AND IMRT PLAN USING INDEPENDENT SOFTWARE) อ.ที่ปรึกษาวิทยานิพนธ์หลัก: รศ. ศิวลี สุริยาปี วศม., อ.ที่ปรึกษาวิทยานิพนธ์ร่วม: ทวีป แสงแห่งธรรม วศด., 65 หน้า.

วัตถุประสงค์ของงานวิจัยนี้เพื่อนำโปรแกรมคำนวณปริมาณรังสีอิสระMuCheck มาตรวจสอบความถูกต้องของการคำนวณปริมาณรังสีด้วยเครื่องวางแผนการรักษา Eclipse ในผู้ป่วยเทคนิคการรักษาแบบ 3D และ IMRT โดยค่าปริมาณรังสีที่คำนวณได้จากMuCheck เปรียบเทียบกับค่าที่วัดในแฟนทอมน้ำโดยตรงก่อน โดยทำการวัดแบบ open และ wedge ในลำรังสีขนาดต่างๆ ตามมาตรฐาน AAPM-TG 53 และ IAEA TRS 430 รวมทั้งทำการวัดปริมาณรังสีเปรียบเทียบสำหรับแผนการรักษาบริเวณสมอง ศีรษะและลำคอ เต้านม และอุ้งเชิงกรานทั้งในเทคนิคการรักษาแบบ 3D และ IMRT จากนั้นโปรแกรม MuCheck จึงถูกนำมาใช้เป็นโปรแกรมอิสระ สำหรับตรวจสอบความถูกต้องของแผนการรักษาผู้ป่วยจริงที่คำนวณจากเครื่องวางแผนการรักษา Eclipse โดยทำการเปรียบเทียบปริมาณรังสีที่จุดอ้างอิงซึ่งมีปริมาณรังสีสม่ำเสมอ ที่บริเวณต่างๆทั่วร่างกาย ผลการทดลองพบว่าความแตกต่างของปริมาณรังสีที่คำนวณได้จากMuCheck และวัดจริงในแฟนทอมน้ำสำหรับ open field, wedge field, เทคนิค 3D, และเทคนิค IMRT อยู่ที่ 2.1%, 2.6%, 1.3%, และ 4.8% ตามลำดับ ในส่วนการประยุกต์ใช้ทางคลินิคจำนวน 301 แผนการรักษาในผู้ป่วยมะเร็งบริเวณสมองศีรษะและลำคอ เต้านม และอุ้งเชิงกรานสำหรับเทคนิคการรักษาและ 3D และ IMRT พบว่าปริมาณรังสีที่คำนวณได้จากโปรแกรม MuCheck แตกต่างจากปริมาณรังสีที่คำนวณได้จากเครื่องวางแผนการรักษา Eclipse ในเทคนิค 3D สำหรับแผนการรักษาบริเวณสมอง เต้านม และอุ้งเชิงกราน อยู่ที่ 2.57 ± 1.16%, 1.85 ± 2.87% และ 1.44 ± 0.84% ตามลำดับ โดยมีค่าเฉลี่ยความแตกต่างรวม 3 บริเวณอยู่ที่ 1.98 ± 1.87% ในส่วนความแตกต่างสำหรับเทคนิค IMRT พบความแตกต่างสำหรับแผนการรักษาบริเวณสมอง ศีรษะและลำคอ เต้านม และอุ้งเชิงกรานที่ 0.85 ± 3.12%, 0.94 ± 3.54%, -1.12 ± 2.30% และ 1.35 ± 2.74% ตามลำดับ โดยมีค่าเฉลี่ยความแตกต่างรวม 4 บริเวณอยู่ที่ 0.52 ± 3.11% จากการทดลองสรุปได้ว่าโปรแกรมอิสระ MuCheck สามารถนำมาใช้ตรวจสอบการคำนวณปริมาณรังสีสำหรับแผนการรักษาผู้ป่วยมะเร็งแบบซับซ้อนได้ทุกบริเวณ ซึ่งจุดที่ใช้คำนวณและเปรียบเทียบควรเป็นจุดที่มีปริมาณรังสีสม่ำเสมอและเป็นจุดที่ตำแหน่งเดียวกัน

ภาควิชา รังสีวิทยา ลายมือชื่อนิสิต .....

สาขาวิชา ฉายาเวชศาสตร์ ลายมือชื่อ อ.ที่ปรึกษาวิทยานิพนธ์หลัก .....

ปีการศึกษา 2556 ลายมือชื่อ อ.ที่ปรึกษาวิทยานิพนธ์ร่วม .....

5574215730 : MAJOR MEDICAL IMAGING
KEYWORDS: PRE-TREATMENT VERIFICATION / PATIENT SPECIFIC QA / MUCHECK / INDEPENDENT DOSE CALCULATION / 3D AND IMRT

VINH CAO HUU: REFERENCE POINT DOSE VERIFICATION IN 3D AND IMRT PLAN USING INDEPENDENT SOFTWARE. ADVISOR: ASSOC. PROF. SIVALEE SURIYAPEE, M.Eng., MR. TAWEAP SANGHANGTHUM, Ph.D., 65 pp.

The purpose of this research is to apply the independent dose calculation for verifying the patient point dose calculated by Eclipse treatment planning system (TPS) in 3D and IMRT techniques as a process of patient specific quality assurance (QA). The MuCheck software was validated by comparing to water phantom measurement for open, wedged fields with the various field sizes as the recommendation of AAPM-TG53 and IAEA-TRS 430. The patient plans in 3D and IMRT for brain, head and neck, breast and pelvis region were randomly chosen from TPS to convert into verification plan and measured in water phantom. After the measurement and MuCheck calculation for basic field and clinical field were verified, the MuCheck software was used as an independent calculation in the real circumstance of treatment for 3D and IMRT in various regions. The point of verification was selected in the uniform dose volume. The limit of confidence of dose differences between MuCheck calculation and measurement in water phantom were within 2.1%, 2.6%, 1.3% and 4.8% for open field, wedged field, composited field in 3D and composite field in IMRT technique, respectively. Clinical application of MuCheck was performed in 301 cases of cancer in brain, head & neck, breast and pelvis regions treated with 3D and IMRT. The clinical use of MuCheck in 3D technique showed the mean difference from Eclipse of 2.57 ± 1.16%, 1.85 ± 2.87%, 1.44 ± 0.84% for brain, breast, and pelvis region, respectively, and 1.98 ± 1.87% for the mean difference of these three treatment regions. The clinical use of MuCheck in IMRT technique showed the dose discrimination from Eclipse of 0.85 ± 3.12%, 0.94 ± 3.54%, -1.12 ± 2.30%, 1.35 ± 2.74% for brain, head & neck, breast and pelvis region, and 0.52 ± 3.11% for the mean of four treatment regions. The MuCheck independent dose calculation software can be employed as a verification tool in patient specific QA for all regions of treatment in advanced treatment techniques. The point dose should be compared point to point between MuCheck calculation and Eclipse calculation in the uniform dose volume.

Department:	Radiology	Student's Signature	.....
Field of Study:	Medical Imaging	Advisor's Signature	.....
Academic Year:	2013	Co-Advisor's Signature	.....

ACKNOWLEDGEMENTS

After two years of learning with the highly serious attitude, this is the time I'm very glad to express my acknowledgement to everybody who has walked with me on the journey seeking the true and knowledge.

First of all, by the most sincere I would like to gratefully thank my advisor, Associate Professor Sivalee Suriyapee for her guidance, understanding, patience, and most important, her friendship during my study at Chulalongkorn University. She encouraged me to not only grow as a worker or physicist but also a researcher, the knowledge must be updated in the whole of my life, and I know that is the useful thing for my long term career as well as my patients in the future.

For every things you have done for me, Dr. Taweap Sanghangthum, I thank you. I have received your enthusiasm, friendship and kindness in helping me doing the thesis.

I would like to thank all of the lecturers, medical physicists, all staffs and oncologists in King Chulalongkorn Memorial Hospital for kind teaching me, especially thank Dr. Taweap Sanghangthum, Mr. Sornjarod Oonsiri, Mrs. Puntiwa Oonsiri have shared with me the knowledge as well as every things in the daily life in Bangkok, from the food to the accommodation. By the friendship, all of you made me feel happy and lessen the homesickness during long time living far away from family.

I would like to thank all of my friends in Master of Science class, especially Mr. Kittipon Dachaworakul, Mr. Phattanapong Saenchon, Mrs. Chitchaya Suwanraksa, Miss Chatnapa Nuntue for their kind helping me in many of procedures; they help my life become simple. I will never forget the time we have learned and joked together.

I deeply thank Associate Professor Anchali Krisanachinda, the chair Medical Imaging Program for supporting me to have the opportunity to take part in this master program.

Finally, I would like to thank University of Medicine and Pharmacy of Ho Chi Minh City, my family and all of my friends for financial support as well as mental support me to finish the course.

CONTENTS

Page

Page

Page

LIST OF TABLES

Page

LIST OF FIGURES

Page

LIST OF ABBREVIATINONS

Abbreviation	Terms
AAMP	The American Association of Physicists in Medicine
ESTRO	European Society for Radiotherapy and Oncology
IDC	Independent Dose Calculation
ICRU	International Commission on Radiation Units and Measurements
MUCV	Monitor Unit Calculation Verification
3D/3DCRT	Three Dimensional Conformal Radiotherapy
IMRT	Intensity Modulated Radiotherapy
PDD	Percentage Depth Dose
SSD	Source–to-Surface Distance
SAD	Source-to-Axis Distance
TPR	Tissue Phantom Ratio
TMR	Tissue Maximum Ratio
TAR	Tissue Air Ratio
BSF	Back Scatter Factor
FOF	Field Output Factor
S_c/COF	Collimator Output Factor
S_p/PSF	Phantom Scatter Factor
TF	Tray Factor
WF	Wedge Factor
ISF	Inverse Square Factor
MF	Mayneord Factor
OAR	Off-Axis Ratio

CHAPTER I
INTRODUCTION

1.1 Background and rationale

According to WHO world cancer trends report, if current trends continue, there will be 22 million new cases of cancer worldwide occurring each year by 2030, this represents an increase of 75% compared with 2008(1). The peoples nowadays face high risk of cancer day by day because of the changes of environment in the modern world. The cancer treatment methods in high technology have been increasing in order to improve the human life. Radiotherapy is one of the major fields of cancer treatment, in which beams of radiation are used to deliver the dose to the patient to kill the tumor while sparing the critical organs surrounded the tumor. With the development of computer science, it allows people developed the treatment planning system (TPS) to calculate the dose delivered to the prescribed target volume (PTV) with the advance treatment technique.

Some different treatment planning systems which are employed to calculate the patient dose mostly for advance treatment techniques such as three-dimensional conformal radiotherapy (3DCRT) or intensity modulated radiation therapy (IMRT) are not only calculated dose at single point but also the dose of a volume. The algorithms used in advance treatment techniques are usually complicated especially for IMRT with many beam angles and intricate intensity maps. The calculated dose from TPS in advance treatment techniques must be verified prior the treatment start to assure that the calculated dose is the same as the prescription dose as well as the actual dose delivers to the patient. The International Commission on Radiation Units and Measurement (ICRU) has recommended in ICRU report 42(2) that the accuracy of calculated dose should be within 2% compared with prescription dose. In the report of the America Association of Physicist in Medicine (AAPM) task group number 114 affirms that the MU verification remains a useful and necessary step in assuring safe and accurate patient treatment (3). The most comprehensive method of verifying the dose delivered to patient is phantom study, in this analysis, the patient plan will be applied in phantom instead of patient and measurements e.g. ion chamber or film dosimetry are employed to verify the calculated dose. However, this process is time consuming and may not be clinically feasible for every patient at the crowded center or at the center where not enough equipment and/or physicist to perform. An alternative method involves the use of

independent dose calculation algorithm to perform the dose verification or monitor unit verification calculation (MUVC), such an MUVC has been recommended in report of AAPM task group 40(4). As mention in AAPM task group 114, nowadays in most institution, MU verification is performed using computer program. This help in cutting down the cost and could reduce the physicist's workload.

The limitations of the dose calculation algorithms exist in all commercial treatment planning systems with a few report of systematic evaluations of these limitations, independent dose calculations (IDC) are also recommended by Dutreixet et al (5) in ESTRO booklet 3. They have been used for a long time as a routine quality assurance (QA) tool in conventional radiotherapy employing empirical algorithms in a manual calculation procedure, or utilizing software based on fairly simple dose calculation. Experimental methods for patient-specific QA in advanced radiotherapy are, however, time consuming in both manpower and accelerator time. As treatment planning becomes more efficient and the number of patients treated with advanced radiotherapy techniques steadily increases, experimental verification may result in a significantly increased workload. Consequently, more efficient methods may be preferred. Independent dose verification by calculation is an efficient alternative and may thus become a major tool in the QA program. There is a growing interest in using calculation techniques for IMRT verification and the commercial products providing IDC tools that can be handled various treatment techniques including IMRT. However, reports and scientific publications that describe their accuracy or other aspects of their clinical application are scarce.

The clinical application of commercial independent dose calculation program of MuCheck on the treatment plan, which is planned by treatment planning system Eclipse, is investigated in this study. Obviously, the algorithms implemented in IDC program and TPS are different, it certainly causes the systematic uncertainties between the plan dose and verification dose, which should be concerned during the investigation. Some different regions of treatment are selected to observe, these are brain, head and neck, breast and pelvis, which are comprehensive in practice.

1.2 Research objective

To verify the patient point doses calculated by Eclipse in 3D and IMRT techniques by comparing with correction-based from MuCheck software.

1.3 The scope of dissertation

- The dose calculation algorithm in treatment planning.

- Point dose verification in radiotherapy treatment planning using independent dose calculation

1.4 Keywords

- Patient specific QA
- Pre-treatment verification
- MuCheck
- Independent dose calculation
- 3D and IMRT.

CHAPTER II
LITERATURES REVIEW

2.1 Theories

2.1.1 Dose calculation parameters

2.1.1.1 Percentage depth dose(6)

Central axis dose inside the patient or phantom are usually normalized to the dose at depth of maximum $D_{z.max}$, 100% at the depth of dose maximum z_{max}. The percentage depth dose is thus defined as follows:

$$PDD(z,A,f,E) = \frac{D_Q}{D_{z\max}} \times 100 = \frac{\dot{D}_Q}{\dot{D}_{z\max}} \times 100 \qquad (2.1)$$

Where: Point Q, which is shown in Figure 2.1, is the arbitrary point in the beam central axis; D_Q and $\dot{D}_Q$ are the dose and dose rate at point Q at depth z on the central axis of the beam. The PDD depends on four parameters: depth in phantom z, field size A, source-to-surface distance (SSD) f, and photon beam energy E.

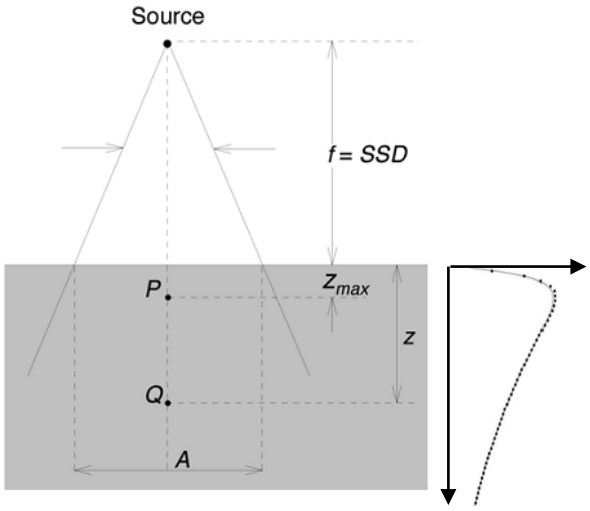

Figure 2.1 Geometry for percentage depth dose measurement and definition

The dose at point Q contains two components: primary (PDD_{pri}) and scatter (K_s)

$$PDD(z,A,f,E) = PDD^{pri} \times K_s \qquad (2.2)$$

— The primary component can be expressed as:

$$PDD^{pri} = \frac{D_Q^{pri}}{D_{z\max}^{pri}} \times 100 = \left(\frac{f + z_{\max}}{f + z}\right)^2 e^{-\mu_{eff}(z - z_{\max})} \quad (2.3)$$

Where μ_{eff} is the linear attenuation for the primary beam in the phantom;

— The scatter component, K_s is a function that accounts for the change in scattered dose, reflects the relative contribution to point Q of scatter radiation.

Since PDD depends on source-to-surface distance f, it must be corrected by a factor called Mayneord F factor if SSD is changed. The Mayneord factor takes into account the variation of SSD from f_1 to f_2 by the relation of equation 2.4

$$F = \left(\frac{f_2 + z_{\max}}{f_1 + z_{\max}}\right)^2 \left(\frac{f_1 + z}{f_2 + z}\right)^2 \quad (2.4)$$

The Mayneord F factor method works reasonably well for small fields since the scattering is minimal under these conditions. However, the method can give rise to significant errors under extreme conditions such as low energy, large field, large depth, and large SSD change.

2.1.1.2 Off-Axis ratio and beam profile(6)

Dose distributions along the beam central axis give only part of the information required for an accurate dose description inside the patient. Dose distributions in 2-dimensions and 3-dimensions are determined with central axis data in conjunction with off-axis dose profiles.

In the simplest form, the off-axis data are given with beam profiles measured perpendicularly to the beam central axis at a given depth in phantom. The depths of measurement are typically at z_{max} and 10 cm for verification of compliance with machine specifications, in addition to other depths required by the particular treatment planning system.

Combining a central axis dose distribution with off-axis data results in a volume dose matrix that provides 2-D and 3-D information of the dose distribution. The off-axis ratio (OAR) is usually defined as the ratio of dose at an off-axis point to the dose on the central beam axis at the same depth in phantom. The curve of OAR is defined as the beam profile at the specified depth that is illustrated in Figure 2.2

$$OAR_x = \frac{D(x, z, A_z, SSD)}{D(0, z, A_z, SSD)} \quad (2.5)$$

Where: x is the distance from the central axis at the depth z with the field size A, OAR_x is the off-axis ratio at the distance x from the central axis

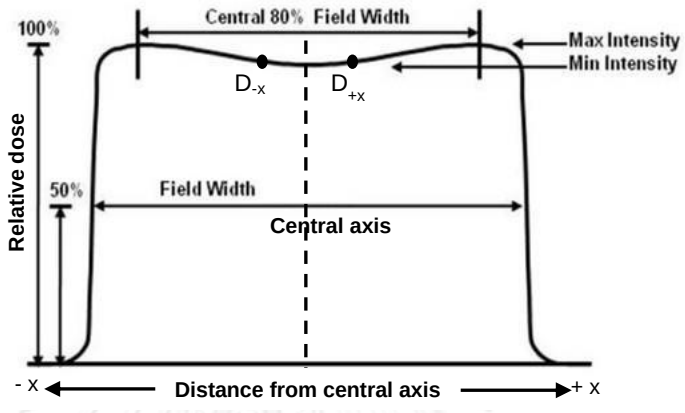

Figure 2.2 An example of beam profile

Dose profile uniformity is usually measured by a scan along the center of both major beam axes for various depths in the water phantom. Two parameters that quantify field uniformity are then determined: beam flatness and beam symmetry.

Beam flatness is assessed by finding the maximum D_{max} and minimum D_{min} dose point values on the profile within the flatness area, 80% of the field width along the major axis, and 60% of the field dimension along the diagonal axis, beam flatness is the ratio of D_{max} to D_{min} expressed as a percentage

$$Flatness = \frac{D_{max}}{D_{min}} \quad (2.6)$$

Beam symmetry is the absolute maximum value of the ratio of the higher to the lower absorbed dose at any two positions symmetrical to the radiation beam axis inside the flattened area, D_{+x} and D_{-x} (where D_{+x} represents the value of the dose at a distance x on one side of the central axis of the beam and D_{-x} is the dose at the corresponding point on the other side of the beam axis)

$$Beam\ symmetry = \frac{D_{+x}}{D_{-x}} \tag{2.7}$$

2.1.1.3 Tissue Phantom Ratio and Tissue Maximum Ratio (6)

The general form of tissue phantom ration, TPR, is defined as the ratio of the dose at a given point on the beam central axis in phantom to the dose at the same point, at a fixed reference depth d_{ref}.

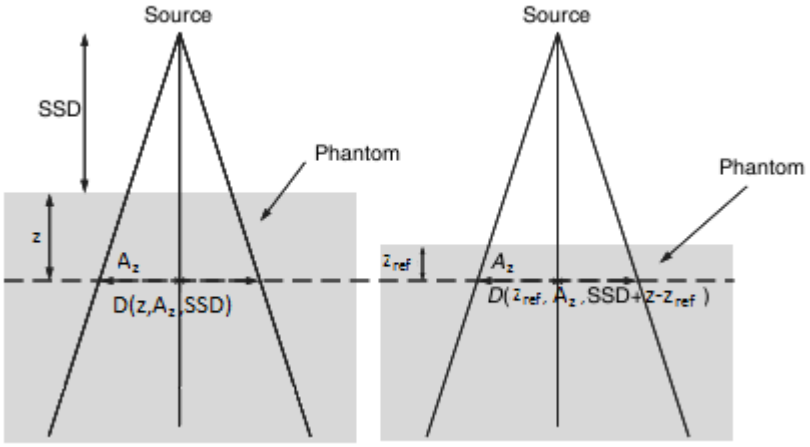

Figure 2.3 Geometry for TPR measurement in phantom

The TPR can be measured by varying the source-to-skin distance (SSD) while keeping the source-to-chamber distance (SCD) constant as illustrated in Figure 2.3. The relation of TPR and the dose presented in formula (1.8) illustrated the independence of TPR from SSD, so that the TPR becomes the megavoltage photon beam quality indicator and the base of the isocentric technique (SAD technique)

$$TPR(z, A_z, E) = \frac{D(z, A_z, SSD, E)}{D(z_{ref}, A_z, SSD_{ref}, E)} \tag{2.8}$$

In which, the TPR for photon beam energy E is measured at depth z with the field size A_z; the reference point is located at the same point but change to SSD_{ref} which is equal to SSD + (Z – Z_{ref}).

A special TPR is defined for the reference depth z_{ref} which is equal to the depth of dose maximum z_{max}, it is referred to as the tissue-maximum ratio TMR (z,A_z,SSD,E)

2.1.1.4 Collimator scatter factor and phantom scatter factor

Measurements of the dose rate (or dose per MU) in phantom as a function of field size, a large number of measurements are required because the dose per MU to a fixed point in a phantom depends on the size of the beam at that point. The measured in-phantom field output factors (FOF) are assumed to be the product of two independent effects: phantom scatter factor (S_p) and collimator (or head) scatter factor (S_c). That is

$$FOF = S_p \times S_c \tag{2.9}$$

The phantom scatter factor (S_p) takes into account the change in scatter radiation originating in the phantom at a reference depth as the field size is changed. S_p may be defined as the ratio of the dose rate for a given field at a reference depth (e.g., depth of maximum dose) to the dose rate at the same depth for the reference field size (e.g., 10 × 10 cm), with the same collimator opening.

As the field size is increased, the output increases because of the increased collimator scatter, which is added to the primary beam. The collimator scatter factor S_c may be defined as the ratio of the output in air for a given field to that for a reference field (e.g., 10 × 10 cm) and may be measured by an ionization chamber with a buildup cap of a size large enough to provide maximum dose buildup for the given energy beam, the setup for measuring collimator scatter factor is shown in Figure 2.4a. and the setup for measuring FOF is shown in Figure 2.4b.

Phantom scatter depends only on the scatter geometry within the phantom or patient; this can be modified by beam shaping, SSD, and patient shape. Collimator (or head) scatter, on the other hand, is independent on the phantom position, but depends on the collimator settings and the presence of additional filters.

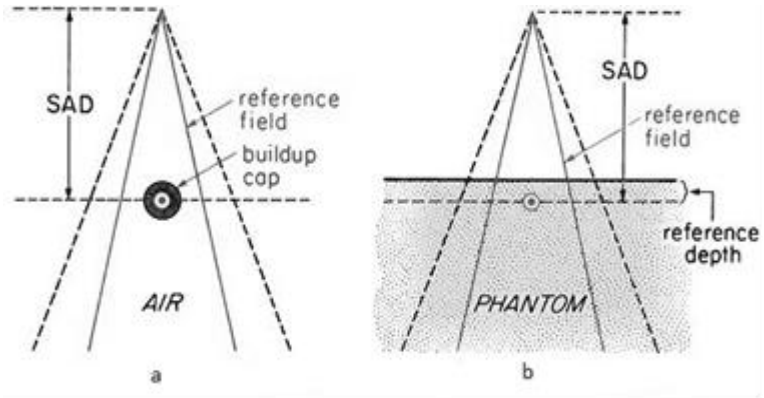

Figure 2.4 Setup geometry for (a) S_c measurement and (b) FOF measurement

2.1.1.5 Tissue air ratio and back scatter factor (6)

Tissue-air ratio, TAR, is defined as the ratio of the dose (D_z) at a given point in the phantom to the dose in free space (D_{fs}) at the same point. This is illustrated in Figure 2.5. For a given quality beam, TAR depends on depth z and field size r_z at that depth:

$$TAR(z, A_z, E) = \frac{D_z}{D_{fs}} \tag{2.10}$$

Since TAR is independent on the SSD, it has been refined to facilitate to calculations for isocentric technique, TAR varies with energy, depth and field size very much.

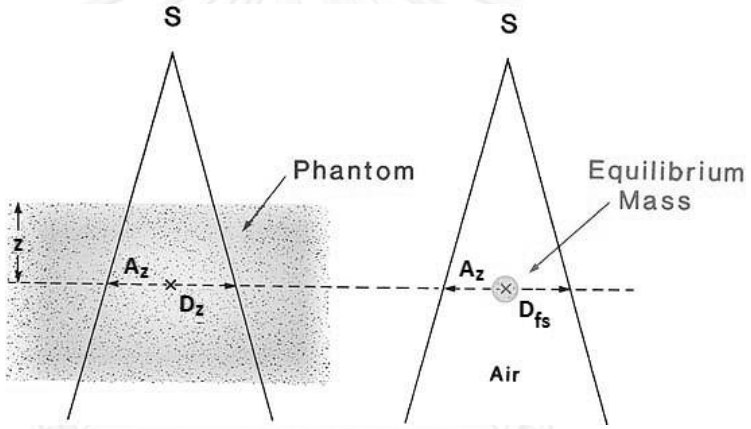

Figure 2.5 Illustration of definition of tissue-air ratio TAR

The term backscatter factor (BSF) is simply the tissue-air ratio at the depth of maximum dose on central axis of the beam. It may be defined as the ratio of the dose on central axis at the depth of maximum dose to the dose at the same point in free space:

$$BSF = TAR(z_{max}, A_{z\,max}, E) = \frac{D_{z\,max}}{D_{fs}} \tag{2.11}$$

2.1.2 Dose calculation algorithms

Computing radiation dose is the most complicated work in radiotherapy, the dose has been measured under specific conditions: given field sizes, fixed depth, homogeneous medium, flat surface; these conditions are not as close as patient conditions. Obviously, the dose must be predicted before beam delivery. To do that, some mathematical models of computations have been released. There are dose

calculation algorithms appropriate with the models, from the simplest conventional to very advanced algorithm. The conventional algorithm – which deployed in independent dose calculation software MuCheck – and the anisotropic analysis algorithm, which implemented in treatment planning system Eclipse, were introduced.

2.1.2.1 Conventional algorithm and Modified Clarkson method (6)

The dose representation of simple beam by the tabulated beam data dose distributions for a number of beams are measured under reference conditions. These data is stored in the tables and are interpolated by the TPS during calculation. The dose is then corrected by the measurement factors so that this method also called correction method. Depend upon the tabulated beam data used; there are two options of dose calculation method using PDD and TMR (or TAR).

Dose calculation using PDD, with the correction of the change in SSD by Mayneord F factor, is shown in equation 2.12. Percentage depth dose is suitable for calculation involving SSD technique, in which the patient was setup base on the source to skin distance.

$$D(z,A,f,E) = K_{@z\max} \times PDD \times (S_p \times S_c) \times TF \times WF \times ISF \times MF \times OAR \qquad (2.12)$$

The dose has been corrected by output factor ($S_p \times S_c$), tray factor TF, wedge factor WF, inverse square factor ISF, Mayneord F factor MF, and off-axis ratio OAR. Where D(z,A,f,E) is the dose per monitor unit (MU) at the point of depth z, $K_{@z.max}$ is the dose per MU at depth of dose maximum in the reference condition (normally be calibrated for 1 cGy/MU).

Dose calculation using TMR (or TAR) is useful for calculations involving isocentric technique of irradiation. Rotation or arc therapy is a type of isocentric irradiation in which the source moves around the axis of rotation, where the tumor is placed. Because the TMR (or TAR) is independent on SSD, the Mayneord F factor has not been used in equation 2.13 and 2.14

$$D(z,A,E) = K_{@z\max} \times TMR_z \times (COF \times PSF) \times TF \times WF \times ISF \times OAR \qquad (2.13)$$

$$D(z,A,E) = K_{@z} \times TAR_z \times (COF \times BSF) \times TF \times WF \times OAR \qquad (2.14)$$

Where; $K_{@z}$ is the dose rate in free space at the calculated point

PDD, TMR (or TAR) and the factors are measured for some reference field sizes and reference depth, so that the interpolation and equivalent square field have been used for other field sizes and depths, that produces the errors of the algorithm.

The PDD and TMR methods remain limitations for irregular shape field, using equivalent square field for irregular field increases the error in calculated dose. To deal with the irregular shape field, the Clarkson method was introduced by Clarkson. Clarkson's method is based on the principle that the scattered component of depth dose, which depends on the field size and shape, can be calculated separately from the primary component; it is independent of the field size and shape. The **Modified Clarkson Integral method** which is based on the concept of Clarkson method is capable of calculating dose for intensity modulated fields. The IMRT field is divided into annular sector (Figure 2.6) in modified Clarkson method and the dose contributed by each annular sector to the point of interest is calculated.

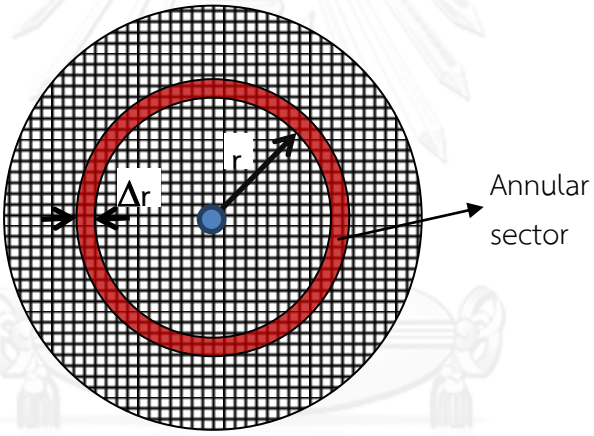

Figure 2.6 Illustration of annular sector of modified Clarkson method

Total dose D_z at the center of an annulus is the sum of primary dose D_P and scattered dose D_S as equation 2.15

$$D_d = D_{P(d)} + D_{S(d)} \tag{2.15}$$

The primary component $D_{P(d)}$ is calculated from $\overline{\mathrm{MU}}_{(0)}$, which is obtained by averaging MU over a small central circular area or zero field size

$$D(z,0,E) = K_{@z,ref} \times \overline{MU}_{(0)} \times TPR_{z(0)} \times \left(COF \times PSF_{(0)}\right) \times ISF \tag{2.16}$$

Where $K_{@z,ref}$ is the dose/MU under reference conditions of calibration at reference depth, $TPR_{z(0)}$ is the tissue-phantom ratio for zero field size at depth z.

The contribution of scattered D_S to central axis at depth z of an annulus between radii r and r + Δr, irradiated by $MU_{(r)}$ is given by:

$$D(z,annulus) = K_{@z\,ref} \times \overline{MU}_{(r)} \times COF \times ISF \times \left[PSF_{(r+\Delta r)} \times TPR_{(r+\Delta r)} - PSF_{(r)} \times TPR_{(r)}\right] \quad (2.17)$$

Where: $\overline{\mathrm{MU}}_{(\mathrm{r})}$ is the average monitor unit over a circular area with the radius r.

The total dose is given by: $\mathrm{D_d} = \mathrm{D_{P(d)}} + \mathrm{D_{S(d)}}$

$$\mathrm{D_d} = \mathrm{K} \times \mathrm{ISF} \times \mathrm{COF} \times \left[\begin{array}{l} \overline{\mathrm{MU}}_{(0)} \times \mathrm{PSF}_{(0)} \times \mathrm{TPR}_{(0)} + \\ +\sum_{\mathrm{r}} \overline{\mathrm{MU}}_{(\mathrm{r})} \times \left[\mathrm{PSF}_{(\mathrm{r}+\Delta\mathrm{r})} \times \mathrm{TPR}_{(\mathrm{r}+\Delta\mathrm{r})} - \mathrm{PSF}_{(\mathrm{r})} \times \mathrm{TPR}_{(\mathrm{r})}\right] \end{array}\right] \quad (2.18)$$

2.1.2.2 Analytical Anisotropic Algorithm(7)

The dose calculation algorithm implemented into the Eclipse (Varian Medical Systems, US) treatment planning system is referred to as analytical anisotropic algorithm (AAA). AAA is a Monte Carlo – base convolution superposition algorithm, the implementation of AAA is split up into a configuration part and a dose calculation part with the multiple source models.

A. The configuration module

The configuration algorithm is used to determine the basic physical parameters to characterize the fluence and energy spectra of the photons and electrons presented in the clinical beam and their fundamental scattering properties in water equivalent medium. These fundamental parameters have been pre-computed with Monte Carlo simulations during beam data configuration so that the resulting calculated beam characteristics match the measured clinical beam data for each treatment unit. The parameters are approximated using a multiple source model: primary photon source, extra-focal radiation source and a third source to model the electron contamination. The parameters specific to the clinical beam are stored in the database and retrieved for patient dose distribution calculation.

For **primary photon source**, the initial photon spectra resulting from bremsstrahlung interaction of the electron beam impinging on the target are pre-calculated using Monte-Carlo methods. The model calculates for mean energy,

intensity profile to take into account the hardening effect of flattening filter and the variation of photon fluence below flattening filter. The optimization of the mean energy and the radial intensity profile should mainly generate correct depth dose curves and profile below the depth of maximum dose.

The extra-focal photon source (second source) models the additional photons generated in the flattening filter, the primary collimator, and the secondary jaws. It is modeled as a virtual source with a finite width located at the bottom plane of the flattening filter. The model derives the mean energy and relative intensity of the extra-focal photon spectrum with the empirical source parameters.

The electron contamination source models the electrons – created mainly by Compton interaction – in the head of the treatment unit and in air. The electron contamination source is viewed as a finite-size source located at the plane of the target. It is modeled by two Gaussians and one energy-deposition function. The total energy deposited by the contaminant electrons as a function of depth in water is modeled by an empirical curve, determined from the difference between the measured depth dose and the depth dose calculated without contaminant electrons for the largest field size.

The above parameters are derived for open beams. Most beam modifying accessories are taken into account in the dose calculation through their impact on the primary photon fluence only. The effect of the beam modifying accessories on the second source and electron contamination source is modeled through their effect on the primary fluence before convolution with the Gaussians.

B. The dose calculation module

The dose calculation is based on separate convolution models for primary photons, scattered extra-focal photons, and electrons scattered from the beam limiting devices. The clinical broad beam is divided into small, finite-sized beamlets (see Figure 2.7) to which the convolutions are applied. The final dose distribution is obtained by the superposition of the dose calculated with photon and electron convolutions for the individual beamlets.

The clinical beam is divided into small beamlets, the patient body volume is divided into a matrix of 3-D voxels along the beamlets, and every voxel is associated with the mean electron density that is computed from CT image according to a user-defined calibration curve.

The clinical beam is represented by two-dimensional fluence distributions describing the incident flux of photon and contamination electron. The final dose distribution is calculated as superposition of the dose deposited by the primary, secondary photons and contamination electron for every beamlets.

The dose deposited by the primary and secondary photons is calculated in the same way with their different spectral composition and focal spot as determined during configuration module of the beam parameters.

A Monte-Carlo integration method is used to construct a set of monoenergetic kernels by calculating pencil beam kernels $h_{E(z,r)}$ for narrow beams of monoenergetic photons of energy E on water phantom; z is the distance from the surface, and r is the orthogonal distance from the central axis. For every beamlet β, a polyenergetic pencil beam kernel $h_{\beta(p)}$ is constructed for every voxel p along the fan line by superposition all the monoenergetic kernels inside beamlet. Figure 2.8 illustrates the pencil beam kernels, beamlet placed in the voxels.

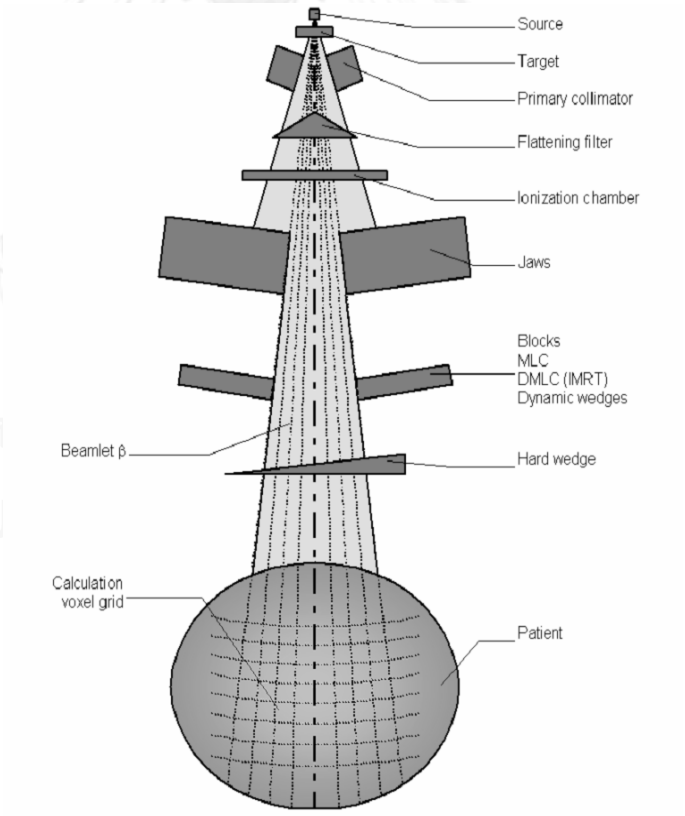

Figure 2.7 Beam unit components, broad beam division

The calculation model separates the energy deposition into depth and lateral component. The depth component $I_{\beta(p)}$ account for the total energy deposition of the pencil beam in layer p_z by the equation 2.19

$$I_\beta(p_z) = \Phi_\beta \iint h_\beta(x, y, p_z)dxdy \tag{2.19}$$

In which, photon fluence Φ_β is assumed to be uniform over the cross section of beamlet.

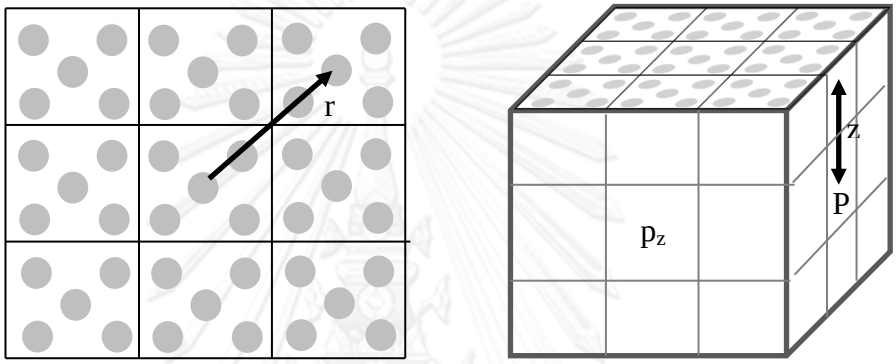

Figure 2.8 Illustration of (a) beamlets and pencil beam kernels, (b) voxels with the pencil beam kernels

The lateral component $k_\beta(\theta,\lambda,p_z)$ in equation 2.20 describes the energy deposited into a very small angular sector at a distance λ from central axis of beamlet for each depth p_z and angle θ

$$k_\beta(\theta, \lambda, p_z) = \sum_{i=1}^{m} c_i \frac{1}{\mu_i} e^{-\mu_i \lambda} \tag{2.20}$$

The lateral component $k_\beta(\theta,\lambda,p_z)$ is modeled as a sum of m radial exponential functions; μ_i is the attenuation coefficient that fixed for each plane, c_i is the weight parameters.

In a homogeneous phantom, the energy deposited by a single beamlet β into a point P, that places in plan p_z, is the product of total energy for this plane and scatter kernel as equation 2.21

$$E_\beta(P) = I_\beta(p_z) \times k_\beta(\theta, \lambda, p_z) \tag{2.21}$$

To account for heterogeneous of patient tissue, the primary and scatter components are scaled by relative electron density

$$\rho_w(P) = \frac{\rho^{el}(P)}{\rho^{el}(water)} \tag{2.22}$$

By applying the relative electron density, the primary component and scatter component become $I'_\beta(p_z)$ and $k'_\beta(\theta, \lambda, p_z)$, with p'_z and λ' are effective depth and effective radius.

$$I'_\beta(p_z) = I_\beta(p'_z)\rho_w(P) \tag{2.23}$$

$$k'_\beta(\theta, \lambda, p_z) = k_\beta(\theta, \frac{p'_z}{p_z}\lambda', p'_z) \times \rho_w(P) \tag{2.24}$$

The final energy deposited into an arbitrary point P from a single beamlet β is computed

$$E'_\beta(P) = I'_\beta(p_z) \times k'_\beta(\theta, \lambda, p_z) \tag{2.25}$$

The total deposited energy in an arbitrary point P is calculated as summation of the contribution of all the individual beamlet

$$E_{tot} = \iint E'_\beta(P) d\beta' \tag{2.26}$$

Finally, the energy distribution is converted to dose distribution by dividing by the local electron density.

Contamination electrons are produced in flattening filter, ion chamber, collimator jaws, air and modifying accessories, the fulence of electron beam Φ_{cont} is model as a convolution of the primary fluence with a Gaussian

$$\Phi_{cont} = \Phi_\beta \otimes G(\sigma_0) \tag{2.27}$$

The dose deposited by the contaminating electrons is then calculated as the convolution of this electron fluence with a second Gaussian multiplied with the electron energy deposition as a function of depth $I(z,p_z)$

$$D_p = \Phi_{cont} \otimes G(\sigma_1) \times I(z, p_z) \quad (2.28)$$

Where: σ_0 and σ_1 are lateral spread of two Gaussians

2.1.3 Three Dimensional Conformal Radiotherapy technique

With computer technology we can see the tumor in three dimensions (3D), width, height and depth, using CT scans or MRI scans. 3DCRT is the treatment technique based on the three-dimension (3D) anatomy information. The information from these scans are fed directly into radiotherapy treatment planning system (TPS), thus doctor can see the treatment area and physicist can design radiation beams base in 3 dimensions of the tumor. Because the treatment volume will be defined in 3D space with many beam directions, physicist can define the treatment volume as closed as possible with PTV. The healthy tissue around the tumor could be spared as much as possible.

In 3D technique, the shape of the tumor can be fitted by block shielding or block multi-leaf collimator (block MLC) for each field of view (FOV) and beam direction. The 3D technique is an excellent treatment option for many types of cancer such as brain cancer, breast cancer, gastrointestinal cancer, lung cancer, gynecologic malignancies. However, this method has its own limitations:

- Lacking of the optimal tools for efficient planning and delivery of conformal radiation therapy.
- Limitation in existing methods of producing desirable radiation dose distribution.

These limitations result in the incorporation of large safety margin to reduce the risk of local relapse. To ensure that unacceptable normal tissue complications are prevented, the tumor dose often has to be maintained at suboptimal level, leading to a higher probability of local failures. Thus, the better localization of extent of the tumor is required. But in case of tumor lies within a region involve healthy tissue, it may not be possible to control the disease at a high enough probability level, without producing normal tissue damage(8).

Therefore, this technique is suitable for simple geometry of tumor and few critical organs surrounding the tumor. For complicate geometry and many critical organs surrounding the tumor, 3D technique cannot spare the healthy tissue so much, this carries people to more advance technique such as IMRT.

2.1.4 Intensity Modulated Radiotherapy technique(6)

Intensity modulated radiation therapy (IMRT) is a sophisticated type of three-dimensional conformal radiotherapy that assigns non-uniform intensities to a tiny subdivision of beams called beamlet. The ability to optimally manipulate the intensities of individual rays within each beam leads to greatly increased control over the overall radiation fluence (i.e. the total number of photons/particles crossing over a given volume per unit time). This in turn allows for the custom design of optimal dose distributions. Improved dose distributions often lead to improved tumor control and reduced toxicity in normal tissue.

When a tumor is not well separated from the surrounding organs at risk and/or has a concave or irregular shape, there may be no practical combination of uniform-intensity beams that will safely treat the tumor and spare the healthy organs. In such instances, adding IMRT to beam shaping allows for much tighter conformity to targets. IMRT requires the setting of the relative intensities of tens of thousands of individual beamlets comprising an intensity modulated treatment plan. This task cannot be accomplished manually and requires the use of a multi-leaf collimator (MLC) and specialized computer assisted optimization methods. A number of computer methods have been devised to calculate optimum intensity profiles, these methods, which are based on inverse planning, can be categorized by analytic method and iterative method (using cost function). However, these methods are beyond the scope of dissertation of this study.

2.1.5 Patient specific quality assurance

The potential of accidents in radiation therapy have been specified in ICRP publication 86(9), one of these is the administration of dose and treatment plan during the treatment. The need of patient specific quality assurance was clarified by Ravichandran(10), in which the patient specific quality assurance was considered as a method to ensure the accuracy in planned and dose delivery in advanced treatment techniques for each individual patient.

Accuracy in planned radiation dose delivery in cancer treatments becomes necessary in the advent of complex treatment delivery options with newer technology using medical linear accelerators, which makes patient management very crucial. Treatment outcome in an individual patient therefore depends on the professional involvement of staff and execution accuracy of planned procedure. The dose of specific patient plan can be performed by measurement in phantom with

ionization chamber, film, diode or in-vivo measurement in patient or independent dose calculation. Each method of verification has its own profits and limitations, the independent calculation was recommended by some literatures (3, 11, 12) for evaluation point dose in patient plan.

2.2 Review of related literatures

Haslam J. J. et al (13) verified the patient dose in IMRT technique using the commercial independent software, RadCalc, to compare with the CORVUS treatment planning system at isocenter. The study was separated into two major sections. The first section, the doses calculated by RadCalc and CORVUS were compared with measurement value. Second section, the variations in dose calculated by CORVUS and RadCalc were analyzed. The mean disparity between CORVUS and RadCalc for entire dataset (507 cases, all of treatment regions) was 1.4% with standard deviation of 1.2%. For each treatment region, the mean percentage differences were 1.4±1.2, 1.6±1.1, 1.1±0.6, 1.2±1.4, 0.2±1.1, 0.6±0.9 for head and neck, prostate, abdomen, miscellaneous, female pelvis, rectum/anus, respectively. This study suggests an acceptable discrepancy between CORVUS and RadCalc of ±3% above the mean value.

Chan J. et al (14) verified the patient dose in 3D technique using "hand" calculation follows the formalism described by Khan [9] to compare with the Pinnacle treatment planning system. The study showed that, the 3D TPS monitor unit calculation was systematically higher than the "hand" calculation by an amount that depended on the complexity of the treatment geometry. For simple geometries the mean difference was 1% and was as high as 3% for more complicated geometries.

Linthout N. et al (15) verified the patient dose in IMRT technique. A spreadsheet was developed to calculate the dose and compare with BrainSCAN treatment planning system. According to the study, the percent dose difference per IMB (Intensity Modulated Beam) was -1.1% with a standard deviation of 6.5% (range from -24.8% to +20.7% and the percent dose difference per treatment was -0.6% with a standard deviation of 2.9% (range from -5.2% to +5.6%). The proposed acceptability levels were ±5.0% or ±2.0 cGy for the percent dose difference per IMB and the absolute dose difference per IMB, respectively. For percent dose difference per treatment, an acceptability level of ±2.0% was proposed.

CHAPTER III
METHODOLOGY

3.1 Materials

This research employs the materials belonging to Division of Therapeutic Radiology and Oncology, King Chulalongkorn Memorial Hospital, Bangkok, Thailand.

3.1.1 Linear accelerator

- Clinac 21EX linear accelerator (Varian Medical Systems, Palo Alto, CA; Figure 3.1), with 80 multi-leaf collimator, is operated in 6 and 10 MV photon beam. The maximum field size of MLC is 40 **x** 40cm^2.

Figure 3.1 Varian Clinac 21EX

- Clinac 23EX and Varian Clinac iX linear accelerators (Varian Medical Systems, Palo Alto, CA) are operated in 6 and 15 MV photon beam (for Clinac 23EX; Figure 3.2) and 6 and 10 MV photon beam (for Clinac iX; Figure 3.3). These models are equipped with 120 individual leaves of MLC for field sizes range from 0.5 x 0.5 cm^2 to 40 x 40cm^2. The central 20 cm of field is shaped by the leaves of 0.5 cm projected width at isocenter and shape 20 cm outer of the field by the leaves of 1.0 cm projected width at isocenter.

Figure 3.2 Varian Clinac 23EX

Figure 3.3 Varian Clinac iX

3.1.2 Electrometer

The DOSE-1 electrometer (IBA dosimetry, Germany; Figure 3.4) is a high precision reference class electrometer. It combines superior accuracy with an excellent resolution in a wide dynamic range (40pC – 1C). It is suitable for the use with ionization chambers, semiconductors and diamond probes.

Figure 3.4 DOSE-1 electrometer

3.1.3 Ionization chambers

- The FC65-P ionization chamber (Wellhofer Dosimetrie, SchwarZenbruck, Germany; Figure 3.5) is a thimble type ion chamber made of Delrin (POM, poly-oxymethylate, 1.425g/cm^2), an aluminum center electrode and a sensitive volume of 0.65 cm^3.
- The CC13 ionization chamber (Wellhofer Dosimetrie, SchwarZenbruck, Germany; Figure 3.6) is designed for scanning applications in computerized water phantom systems, high spatial resolution features with small sensitive volume of 0.13cm^3.

Figure 3.5 FC65-P ionization chamber

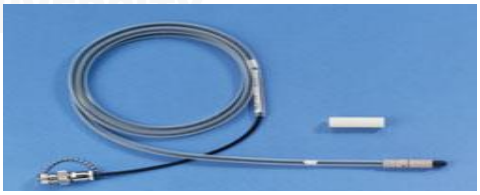

Figure 3.6 CC13 ionization chamber

3.1.4 Water phantom

The WP1D water phantom (IBA dosimetry, Germany; Figure 3.7) is a 1D stand-alone water phantom for absolute dose measurements according to TG-51 and IAEA TRS-398 dosimetry protocols. This study uses the WP1D water phantom with the

Motorized water phantom including Smart Control Unit (SCU): which the measurement depth can be adjusted in steps of 0.1-100 mm.

Figure 3.7 WP1D water phantom

3.1.5 Treatment planning system

The Eclipse version 8.9.21 (Varian medical systems; Figure 3.8) is a primary treatment planning software, which can plan any treatment technique for both photon beam and electron beam. For photon beam, a new photon dose calculation model, the Analytical Anisotropic Algorithm (AAA) has been implemented(7).

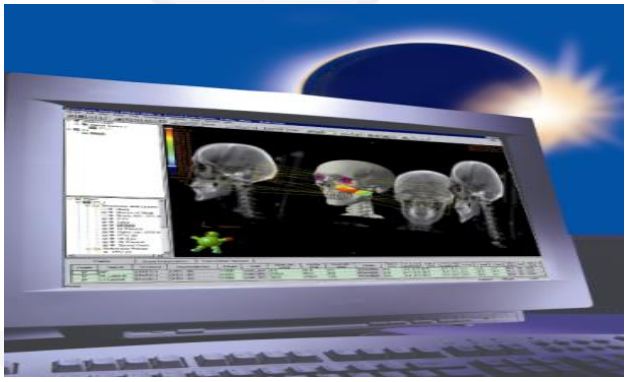

Figure 3.8 Eclipse treatment planning software

3.1.6 Independent dose calculation software

The MuCheck software (Oncology Data Systems, Inc; Figure 3.9) has been designed as a second-check verification tool to assure monitor unit calculations. The software has been validated by FDA on Jun-8-1998 (16). This calculation program can be input to the treatment plans by importing directly from DICOM file; it is convenient for computing the dose in 3D and IMRT techniques.

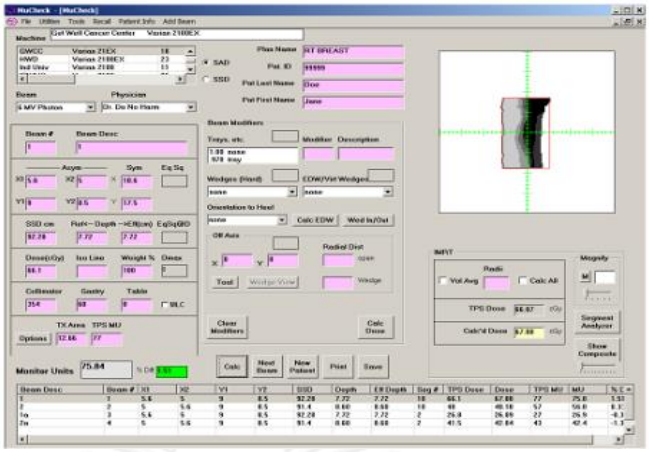

Figure 3.9 MuCheck software

3.1.7 Clinical treatment plan

Patient treatment plans of 3D and IMRT techniques are collected from computer system. The 301 plans are collected, in which 127 plans of 3D and 174 plans of IMRT are considered. The plans are categorized by treatment regions involving brain, head and neck, breast, and pelvis.

- The 46 plans of brain, 40 plans of breast and 41plans of pelvis are investigated for 3D technique.
- The 43 plans of brain, 48 plans of head and neck, 42 plans of breast and 41 plans of pelvis are investigated for IMRT technique.

3.2 Methods

3.2.1 Conceptual framework

The patient dose delivered to patient is affected by many factors such as the beam data, treatment techniques, calculation algorithms, regions of treatment and some other factors. In the clinical aspect, the factors that should be paid attention are the treatment techniques, treatment regions and the calculation algorithms.

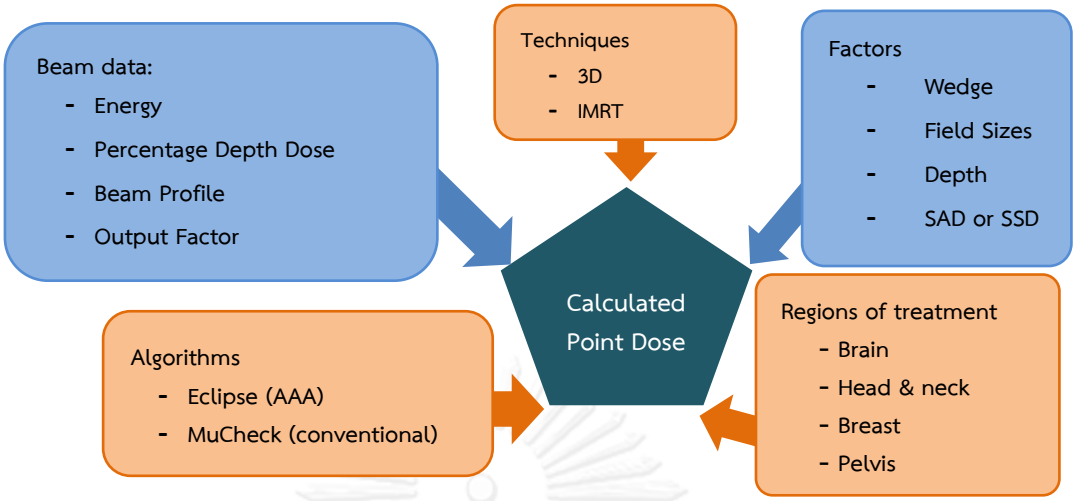

Figure 3.10 Conceptual framework

3.2.2 Research design

This research is designed as an observational descriptive study, the discrepancies of the dose difference between independent dose calculation program and treatment planning system are observed to verify the patient point doses. The process is followed the steps shown in Figure 3.11.

3.2.3 Research design model

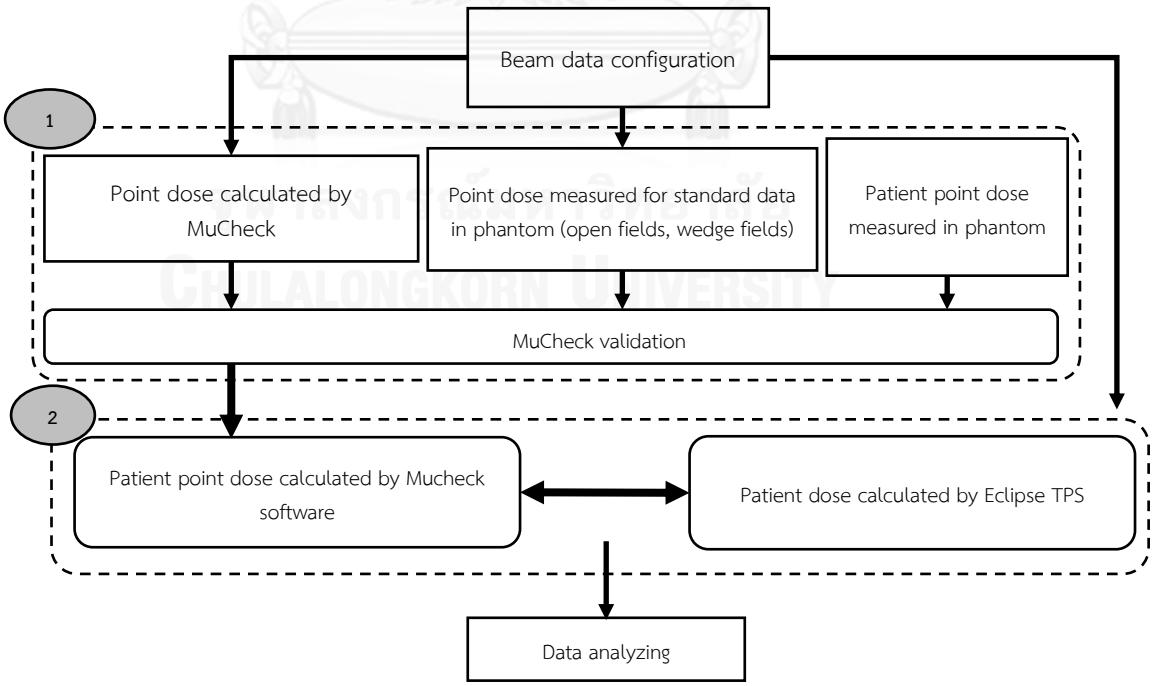

Figure 3.11 Research design model

3.2.4 Validation of independent software by measurement in water phantom

3.2.4.1 Beam output correction

The beam outputs were measured using ion chamber, to obtain the absolute dose correction factor (CF) for 1 cGy/MU at the point of dose maximum using the equation 3.1. The practical setup of beam output correction is shown in Figure 3.12; the IC was set at 10 cm depth, 100 cm SSD with the field size of 10x10 cm^2.

$$CF = \frac{1(cGy/MU)}{D_{max}(cGy/MU)} \tag{3.1}$$

The absolute dose was determined following the IAEA TRS 398(17) protocol and converted to the dose at depth of maximum D_{dmax} using PDD. Then the equation 3.1 was applied.

The correction is done for all energies of accelerators.

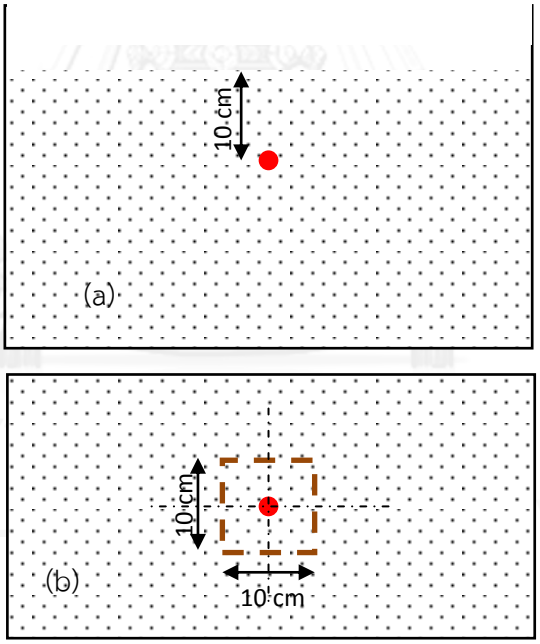

Figure 3.12 Practical setup for output correction (a) side view, (b) top view

3.2.4.2 Measurement in phantom

Before using MuCheck in the clinic, the software has been validated by comparing with phantom measurement. The measurements were performed in water phantom with the basic field sizes as well as the patient plan.

Table 3.1 shows the basic field sizes of open and wedge fields that recommended by some previous literatures (18, 19). The patient plans were randomly selected from TPS, converted into verification plan and measured in water phantom for brain, head and neck, breast and pelvis region. The fields of verification plan were reset at zero- angle of gantry, collimator and couch. The ionization chamber was set at 5 cm depth as shown in Figure 3.13 for all of the measurements.

The reading M(nC) was converted to the dose by the correction factor as equation3.2. The point of verification was selected at the isocenter.

$$D = CF \times M\left(nC\right) \times N_{D,w}\left(\frac{cGy}{nC}\right) k_s k_Q k_{TP} k_{pol} \qquad (3.2)$$

Where, $N_{D,w}$ is the calibration factor, and k_s, k_Q, k_{TP}, k_{pol} are the correction factors for ionization recombination, beam quality, temperature/pressure, polarity effect, respectively.

Table 3.1 The fields sizes of dose measurement in phantom for open and wedged fields

Field types		Field sizes (cm^2)
Open	Square *	5x5, 8x8, 10x10, 20x20, 30x30
	Rectangular **	4x7, 7x4, 7.5x15, 15x7.5, 5x30, 30x5
Wedged	15°	5x5, 10x10, 20x20
	45°	5x5, 10x10, 20x20

* Refer to AAPM TG53 **(18)**, **Refer to IAEA TRS 430 **(19)**

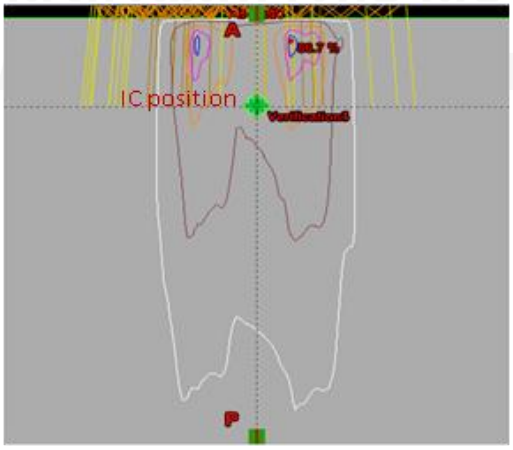

Figure 3.13 The IMRT verification plan in water phantom with zero degree of gantry, collimator and couch converted form patient plans

The percentage of dose difference between measurement and MuCheck calculation was computed by equation 3.3

$$\%diff = \frac{\left(D_P^{MuCheck} - D_P^{Measurment}\right)\times 100}{D_P^{Measurment}} \quad (3.3)$$

Where D_P was the dose calculated or measured at point P

3.2.5 Clinical application of independent software

The application of clinical plan was performed for the actual circumstance of treatment. The plans of brain, head and neck, breast, pelvis regions were selected for 3D (127 cases) and IMRT techniques (174 cases). The point of dose verification was created on the plan should be placed at the uniform dose volume. The plans then were exported from TPS in DICOM file and imported to MuCheck software to calculate the dose at selected point. The percentage of dose difference was computed as the equation 3.4

$$\%diff = \frac{\left(D_P^{MuCheck} - D_P^{Eclipse}\right)\times 100}{D_P^{MuCheck}} \quad (3.4)$$

The verification point P in the independent software must be the same location as the verification point in the treatment plan. The dose was compared point to point in MuCheck and TPS.

3.2.5.1 Statistical analysis

The difference in the dose was investigated between calculated by MuCheck independent software and Eclipse treatment planning system by equation 3.4. The data were analyzed for the mean, standard deviation and the confident limit as the equation 3.5, 3.6 and 3.7(20)

$$\bar{x} = \frac{\sum_i x_i}{n} \quad (3.5)$$

$$SD = \left[\frac{\sum_i \left(x_i - \bar{x}\right)^2}{n-1}\right]^{1/2} \quad (3.6)$$

$$\Delta = |\bar{x}| + 1.5SD \tag{3.7}$$

Where: x was the dose difference; SD was the standard deviation and Δ was the limit of confident. The 1.5SD was recommended by Venselaar et al(21).

The data analysis has been done by Microsoft Excel.

CHAPTER IV
RESULTS

4.1 Validation of independent software by measurement water phantom

4.1.1 Beam output calibration correction

4.1.1.1 Output calibration correction with FC-65P ion chamber for 6MV photon in Clinac iX

SSD: 100 cm

Depth: 10 cm

Field size: 10×10 cm^2

Temperature: 21.3 ^{o}C

Pressure: 1011.5 mbar

Ion chamber calibration factor: 4.889 cGy/nC

Table 4.1 Ion chamber reading for dose calibration correction with FC-65P for 6MV photon in Clinac iX

Voltage	Reading (nC)			Average reading (nC)
+300	13.66	13.66	13.67	13.66
+100	13.60	13.59	13.59	13.59
-300	13.70	13.69	13.70	13.70

Temperature/pressure correction factor k_{TP}: 1.00617

Ion recombination correction factor k_s: 1.00248

Polarity effect correction factor k_{pol}: 1.00122

Beam quality correction factor $k_{Q,Qo}$: 0.9939

Dose at depth of 10 cm D_{10cm}: 0.6705 cGy/MU

Dose at depth of maximum $D_{z,max}$: 1.0113 cGy/MU

Output calibration correction with FC-65P IC for 6MV photon is 0.9888

4.1.1.2 Output calibration correction with FC-65P ion chamber for 10MV photon in Clinac iX

SSD: 100 cm

Depth: 10 cm

Field size: 10×10 cm^2

Temperature: 21.3 $^{\circ}C$

Pressure: 1011.5 mbar

Ion chamber calibration factor: 4.889 cGy/nC

Table 4.2 Ion chamber reading for dose calibration correction with FC-65P for 10MV photon in Clinac iX

Voltage	Reading (nC)			Average reading (nC)
300	15.24	15.25	15.26	15.25
100	15.11	15.11	15.13	15.12
-300	15.25	15.24	15.24	15.24

Temperature/pressure correction factor k_{TP}: 1.00617

Ion recombination correction factor k_s: 1.00428

Polarity effect correction factor k_{pol}: 0.99978

Beam quality correction factor $k_{Q,Qo}$: 0.98154

Dose at depth of 10 cm D_{10cm}: 0.7393 cGy/MU

Dose at depth of maximum $D_{z,max}$: 1.0099 cGy/MU

Output calibration correction with FC-65P IC for 10MV phton is 0.9901

4.1.1.3 Output calibration correction with CC13 ion chamber for 6MV photon in Clinac iX

SSD: 100 cm

Depth: 10 cm

Field size: 10×10 cm^2

Temperature: 21.3 $^{\circ}C$

Pressure: 1011.5 mbar

Ion chamber calibration factor: 26.46 cGy/nC

Table 4.3 Ion chamber reading for dose calibration correction with CC13 for 6MV photon in Clinac iX

Voltage	Reading (nC)			Average reading (nC)
300	2.507	2.506	2.505	2.506
100	2.479	2.481	2.483	2.481
-300	2.507	2.507	2.509	2.507

Temperature/pressure correction factor k_{TP}: 1.00617

Ion recombination correction factor k_s: 1.00490

Polarity effect correction factor k_{pol}: 1.00033

Beam quality correction factor $k_{Q,Qo}$: 0.99490

Dose at depth of 10 cm D_{10cm}: 0.667 cGy/MU

Dose at depth of maximum $D_{z,max}$: 1.00641 cGy/MU

Output calibration correction with CC13 IC for 6MV photon is 0.9936

4.1.1.4 Output calibration correction with CC13 ion chamber for 10MV photon in Clinac iX

SSD: 100 cm

Depth: 10 cm

Field size: 10×10 cm^2

Temperature: 21.3 $^{\circ}C$

Pressure: 1011.5 mbar

Ion chamber calibration factor: 26.46 cGy/nC

Table 4.4 Ion chamber reading for dose calibration correction with CC13 for 10MV photon in Clinac iX

Voltage	Reading (nC)			Average reading (nC)
300	2.79	2.789	2.788	2.789
100	2.759	2.761	2.758	2.759
-300	2.795	2.794	2.791	2.793

Temperature/pressure correction factor k_{TP}: 1.00617

Ion recombination correction factor k_s: 1.00523

Polarity effect correction factor k_{pol}: 1.00078

Beam quality correction factor $k_{Q,Qo}$: 0.98475

Dose at depth of 10 cm D_{10cm}: 0.7356 cGy/MU

Dose at depth of maximum $D_{z,max}$: 1.00491 cGy/MU

Output calibration correction with CC13 IC for 10MV photon is 0.9951

4.1.1.5 Output calibration correction with CC13 ion chamber for 15MV photon in Clinac 23EX

SSD: 100 cm

Depth: 10 cm

Field size: 10×10 cm^2

Temperature: 23 ^{o}C

Pressure: 1008 mbar

Ion chamber calibration factor: 26.46 cGy/nC

Table 4.5 Ion chamber reading for dose calibration correction with CC13 for 15MV photon in Clinac 23EX

Voltage	Reading (nC)			Average reading (nC)
300	2.846	2.844	2.846	2.845
100	2.794	2.792	2.792	2.793
-300	2.849	2.848	2.846	2.848

Temperature/pressure correction factor k_{TP}: 1.01550

Ion recombination correction factor k_s: 1.00927

Polarity effect correction factor k_{pol}: 1.00041

Beam quality correction factor $k_{Q,Qo}$: 0.9797

Dose at depth of 10 cm D_{10cm}: 0.7563 cGy/MU

Dose at depth of maximum $D_{z,max}$: 0.9873 cGy/MU

Output calibration correction with CC13 IC for 15MV photon is 1.0129

4.1.2 Validating software by measuring basic field size in water phantom

The measurements were performed in water phantom using FC – 65P ion chamber placed at the depth of 5 cm and SSD of 100 cm. The open and wedged fields with the field size that recommended in Table 3.1, and the composite fields for 3D and IMRT were investigated using FC – 65P and CC – 13 ion chamber, respectively. The ion chamber readings were converted to the dose using equation 3.2 and compared to the calculated dose from independent dose calculation software, MuCheck. The data of comparison between MuCheck and measurement is shown in Appendix A.

4.1.2.1 The open field measurement

The open field measurement in water phantom revealed that the dose difference between MU check calculation and measurement ranged from -2.4% to 3.0%. The average dose difference was 0.1 $\pm$ 1.3% with the confident limit of 2.1% (1.5SD). The frequency of percentage difference is shown in Figure 4.1 and the bar chart in Figure 4.2 presents the data of dose difference between MuCheck and measurement.

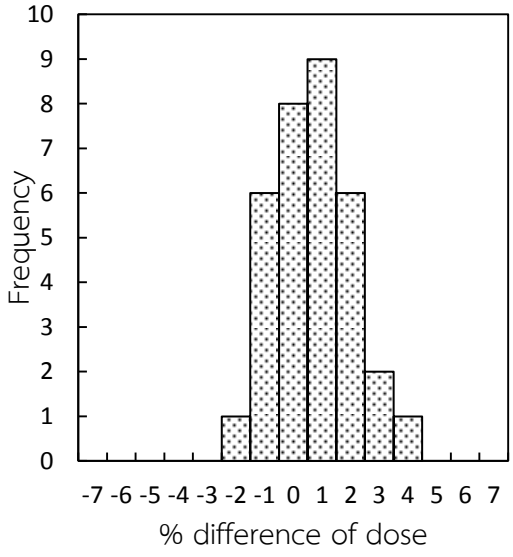

Figure 4.1 The distribution histogram of percentage dose difference between MuCheck and phantom measurement for open field

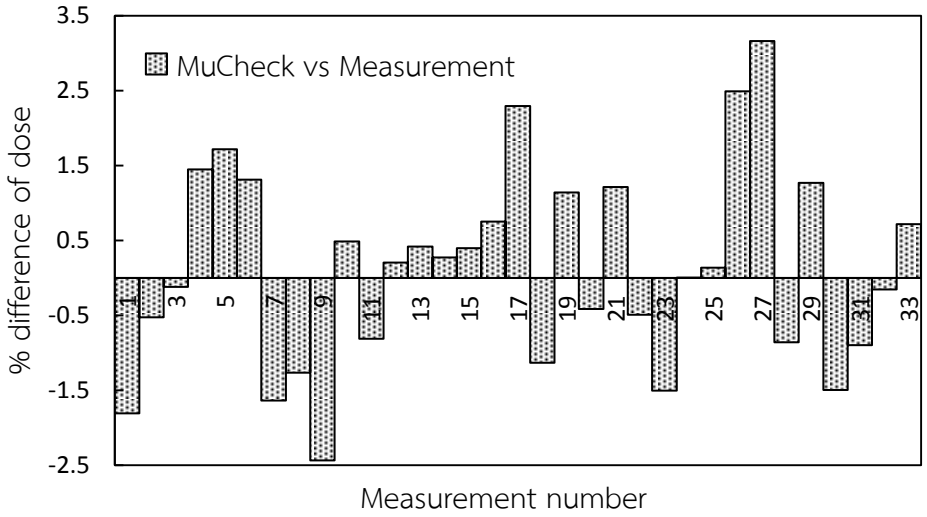

Figure 4.2 The dose difference between MuCheck and measurement for open field

4.1.2.2 The wedged field measurement

The wedged field measurement in water phantom showed the range of dose difference from -2.2% to 3.5%. The average dose difference was 0.4 ± 1.5% with the confident limit of 2.6% (1.5SD). The frequency of percentage difference is shown in Figure 4.3 and the bar chart in Figure 4.4 presents the data of dose difference between MuCheck and measurement.

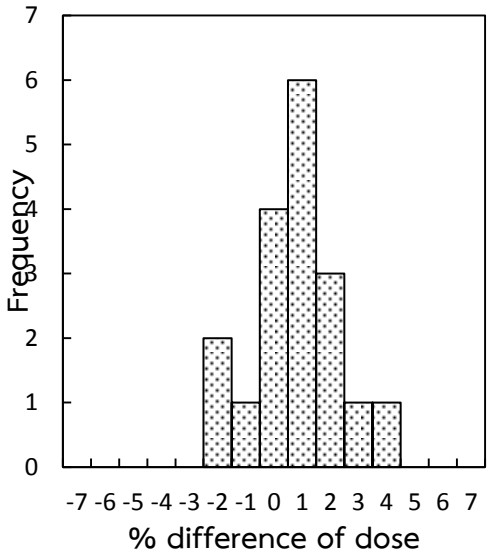

Figure 4.3 The distribution histogram of percentage dose difference between MuCheck and phantom measurement for wedged field

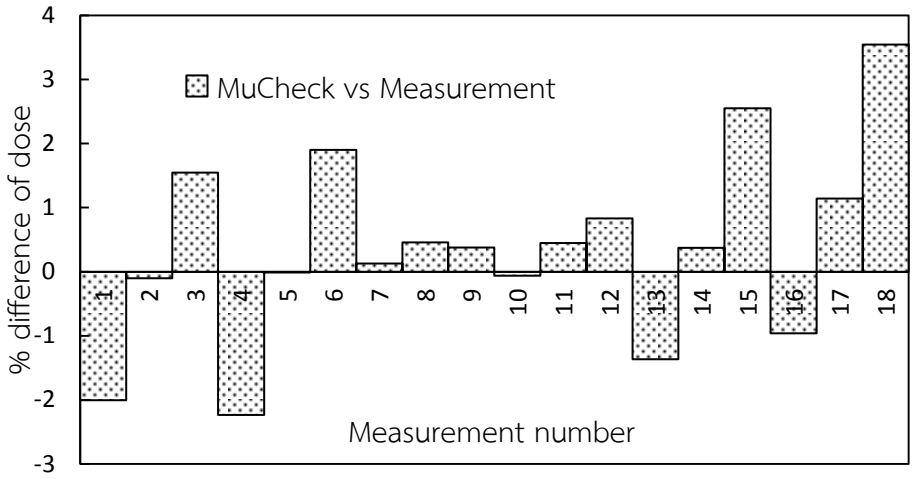

Figure 4.4 The dose difference between MuCheck and measurement for wedged field

4.1.2.3 The composite field in 3D technique measurement

The 15 composite fields in 3D technique which were measured in water phantom showed the range of dose difference from -1.3% to 1.2%. The average dose difference was 0.2 $\pm$ 0.7% with the confident limit of 1.3% (1.5SD). The frequency of percentage difference is shown in Figure 4.5 and the bar chart in Figure 4.6 presents the data of dose difference between MuCheck and measurement.

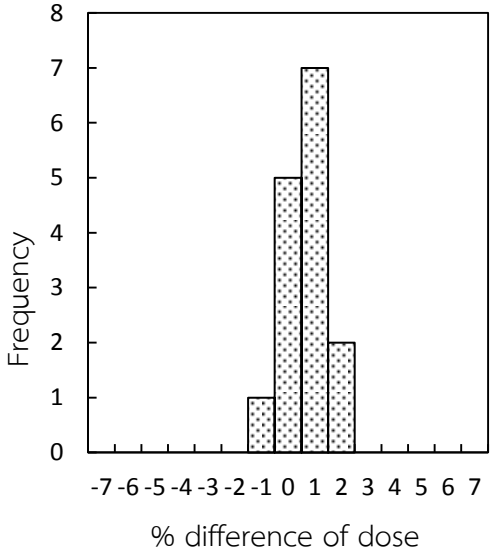

Figure 4.5 The distribution histogram of percentage dose difference between MuCheck and phantom measurement for composite field in 3D technique

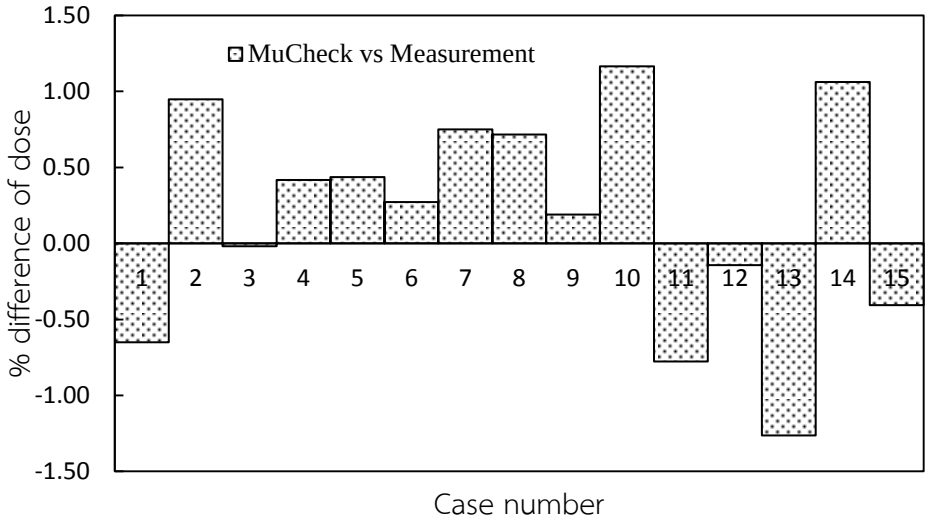

Figure 4.6 The dose difference between MuCheck and measurement for composite field in 3D technique

4.1.2.4 The composite field in IMRT technique measurement

The 41 composite fields in IMRT technique are measured in water phantom showed the range of dose difference from -5.5% to 5.0%. The average dose difference was -0.2 $\pm$ 2.7% with the confident limit of -4.8% (1.5SD). The frequency of percentage difference is shown in Figure 4.7 and the bar chart in Figure 4.8 presents the data of dose difference between MuCheck and measurement.

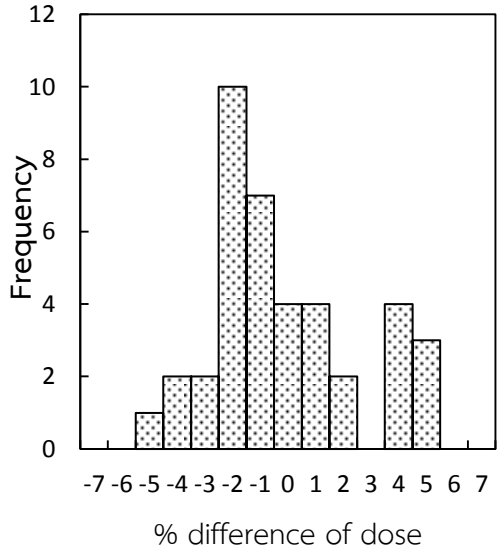

Figure 4.7 The distribution histogram of percentage dose difference between MuCheck and phantom measurement for composite field in IMRT technique

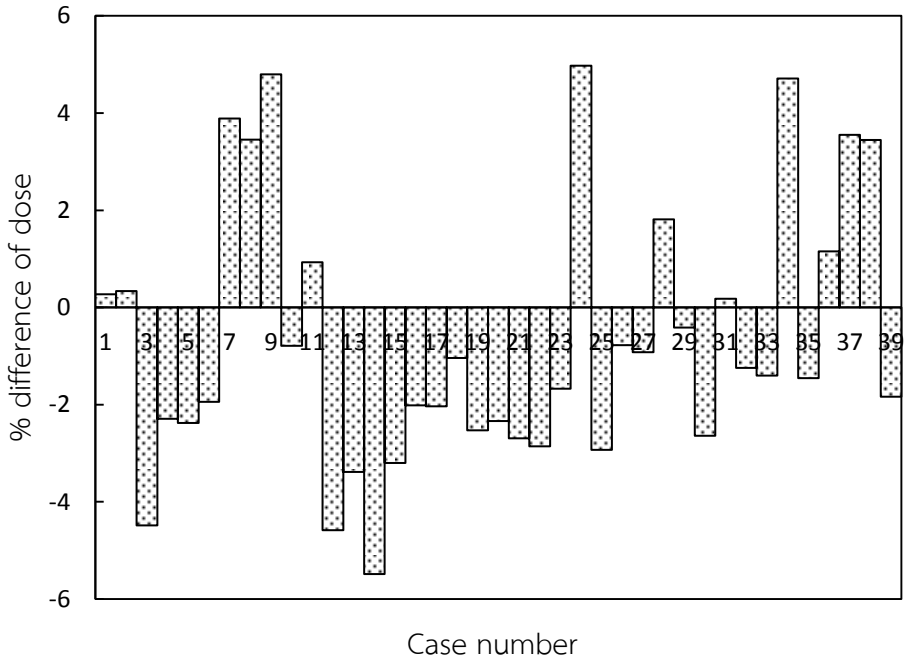

Figure 4.8 The dose difference between MuCheck and measurement for composite field in IMRT technique

4.2 Clinical application of independent software

The independent calculation was applied in clinical plans for brain, breast, and pelvis region in 3D technique, for brain, head and neck, breast, and pelvis region in IMRT technique. The patient plans were exported to DICOM file from TPS and imported to MuCheck to compute the dose at the verification point. All the data of clinical application are presented in Appendix B and Appendix C.

4.2.1 Three Dimensional Conformal Radiotherapy

4.2.1.1 Brain region in 3D technique

The 46 cases of brain plans were investigated; the mean of dose difference of MuCheck from Eclipse was 2.57 $\pm$ 1.16%. The discrepancy of MuCheck from Eclipse is shown in Figure 4.9 and its distribution that is presented in Figure 4.10 indicated the range of the discrepancy from -0.54% to 4.71%.

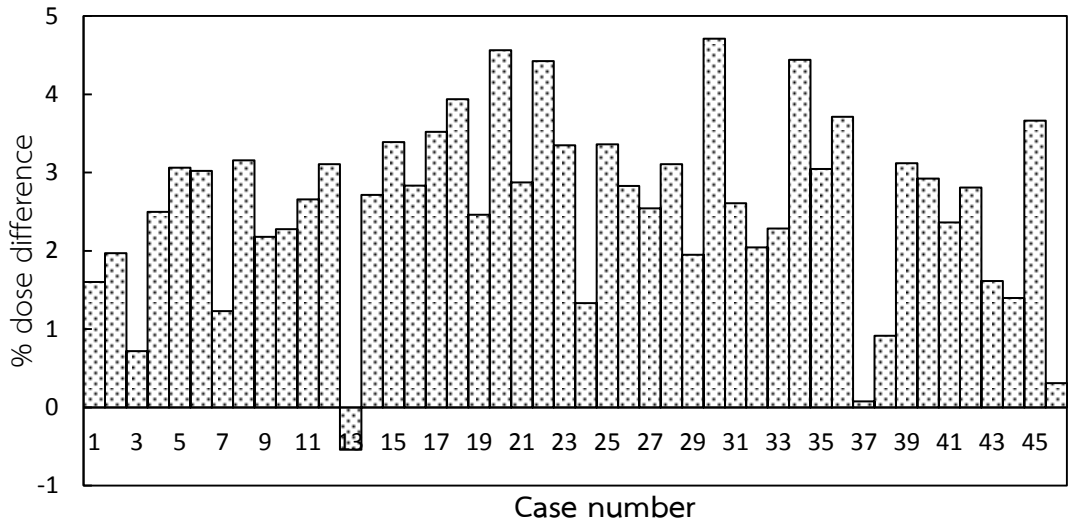

Figure 4.9 The dose difference between MuCheck and Eclipse for brain region in 3D technique

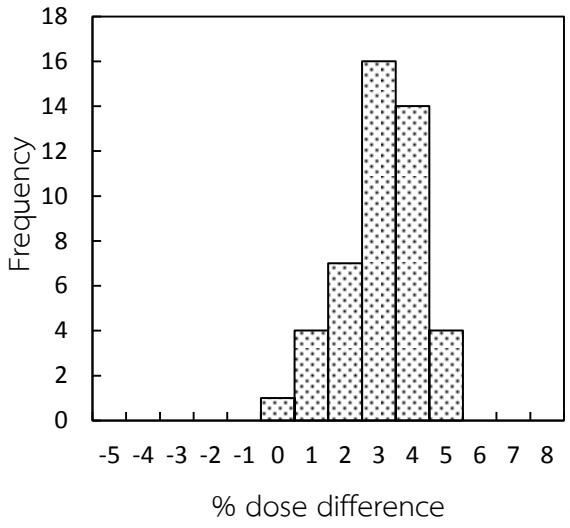

Figure 4.10 The distribution histogram of percentage dose difference between MuCheck and Eclipse for brain in 3D technique

4.2.1.2 Breast region in 3D technique

The 40 cases of breast were investigated; the mean of dose difference of MuCheck from Eclipse was 1.85 $\pm$ 2.87%. The discrepancy of MuCheck from Eclipse is shown in Figure 4.11 and its distribution that is presented in Figure 4.12 indicated the range of the discrepancy is from -6.14% to 5.21%

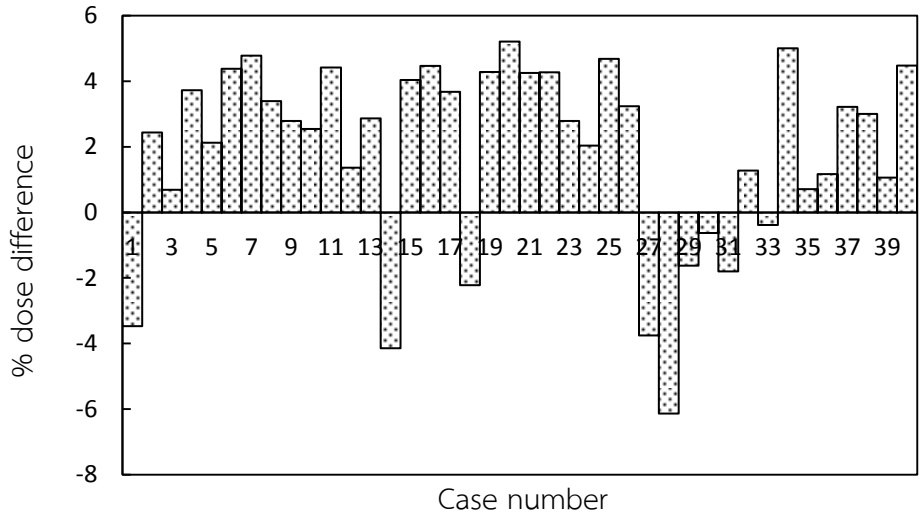

Figure 4.11 The dose difference between MuCheck and Eclipse for breast region in 3D technique

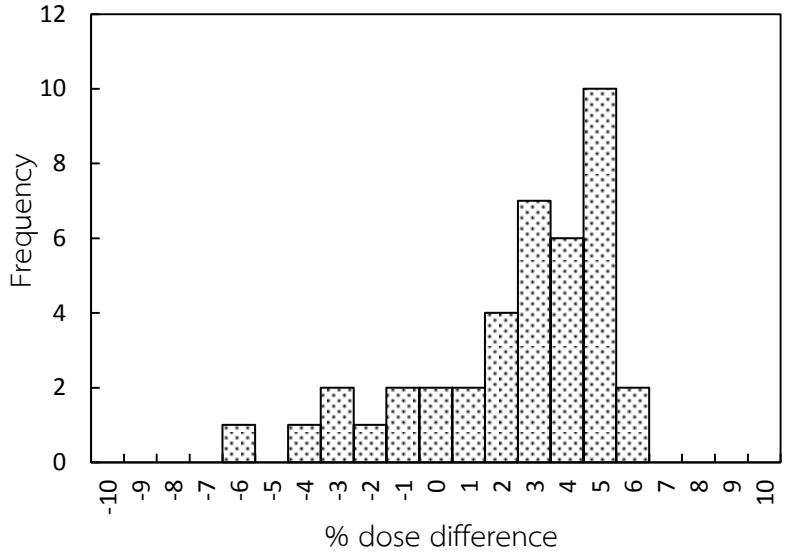

Figure 4.12 The distribution histogram of percentage dose difference between MuCheck and Eclipse for breast region in 3D technique

4.2.1.3 Pelvis region in 3D technique

The 41 cases of pelvis region were investigated; the mean of dose difference of MuCheck from Eclipse was 1.44 $\pm$ 0.84%. The discrepancy of MuCheck from Eclipse is shown in Figure 4.13 and its distribution that is presented in Figure 4.14 indicated the range of the discrepancy from -1.37% to 3.16%.

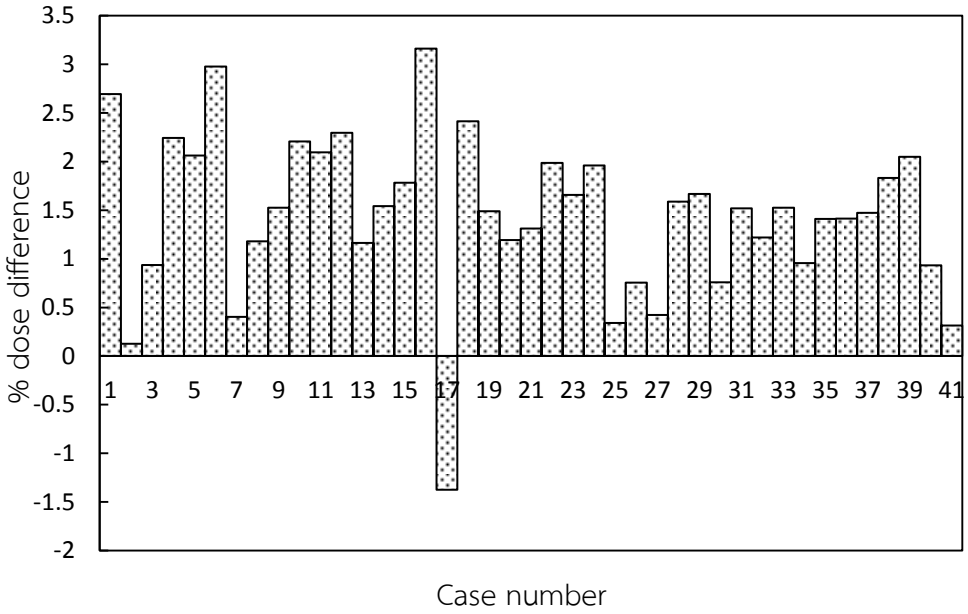

Figure 4.13 The dose difference between MuCheck and Eclipse for pelvis region in 3D technique

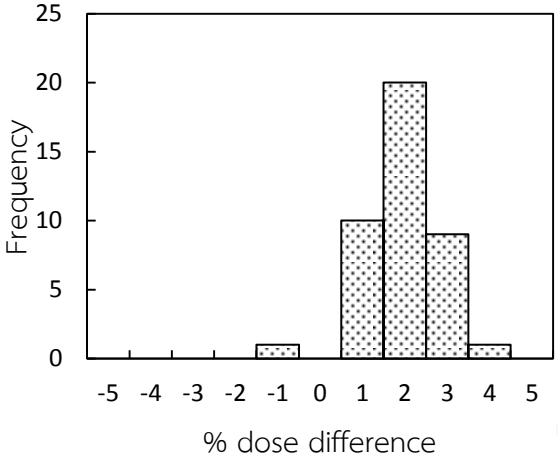

Figure 4.14 The distribution histogram of percentage dose difference between MuCheck and Eclipse for pelvis region in 3D technique

4.2.1.4 All of treatment regions in 3D technique

The 127 cases of 3D plan for brain, breast and pelvis regions were investigated; the mean of dose difference of MuCheck from Eclipse was 1.98 $\pm$ 1.87%. The distribution of dose difference is presented in Figure 4.15.

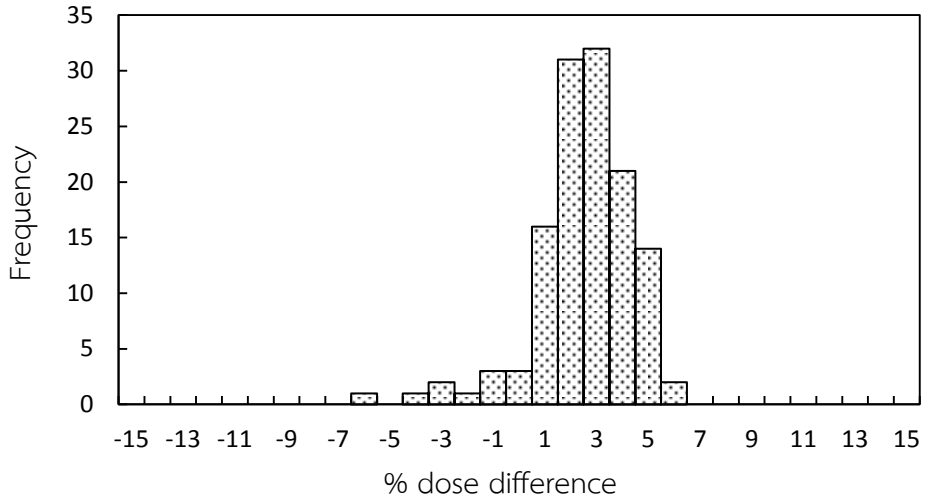

Figure 4.15 The distribution histogram of percentage dose difference between MuCheck and Eclipse in 3D technique for all regions

4.2.2 Intensity Modulated Radiotherapy

4.2.2.1 Brain region in IMRT technique

The 43 cases of IMRT brain region were investigated; the mean of dose difference of MuCheck from Eclipse was 0.85 $\pm$ 3.12%. The discrepancy of MuCheck from Eclipse is shown in Figure 4.16 and its distribution that is presented in Figure 4.17 indicated the range of the discrepancy is from -3.44% to 8.60%.

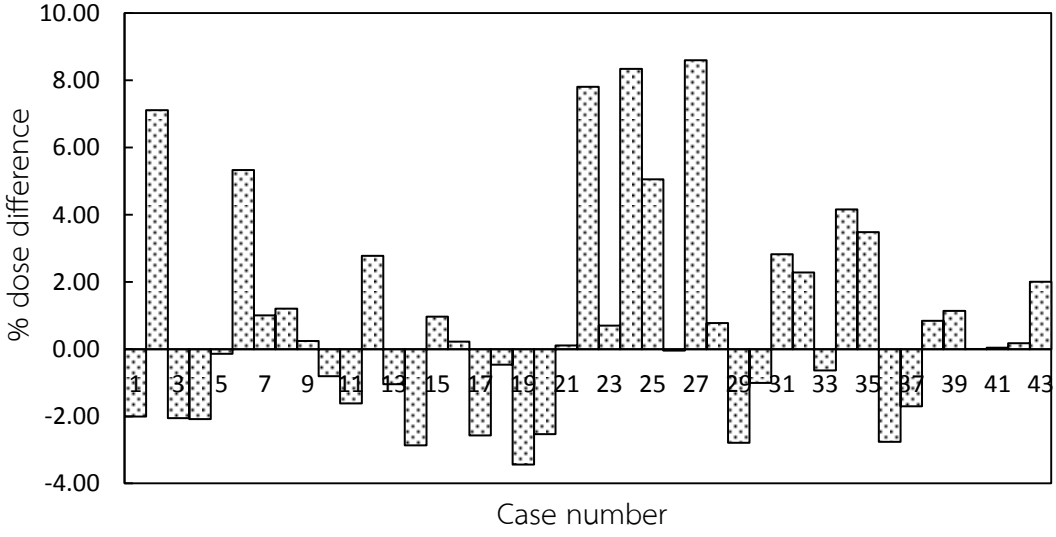

Figure 4.16 The dose difference between MuCheck and Eclipse for brain region in IMRT technique

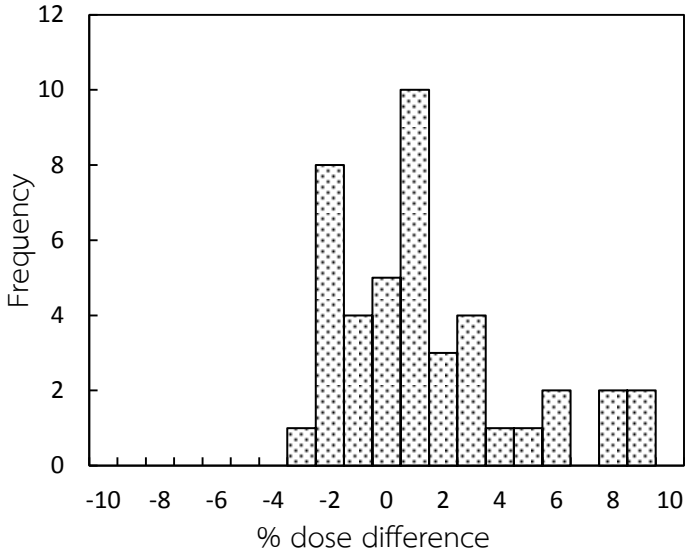

Figure 4.17 The distribution histogram of percentage dose difference between MuCheck and Eclipse for brain region in IMRT technique

4.2.2.2 Head and neck region in IMRT technique

The 48 cases of IMRT head and neck region were investigated; the mean of dose difference of MuCheck from Eclipse was 0.94 $\pm$ 3.54%. The discrepancy of MuCheck from Eclipse is shown in Figure 4.18 and its distribution that is presented in Figure 4.19 indicates the range of the discrepancy from -6.41% to 7.45%

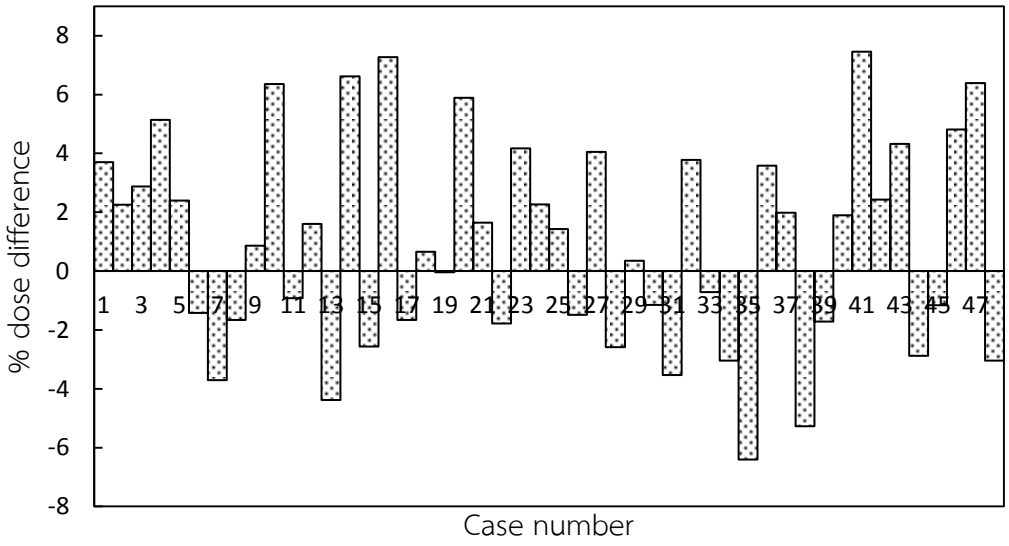

Figure 4.18 The dose difference between MuCheck and Eclipse for head and neck region in IMRT technique

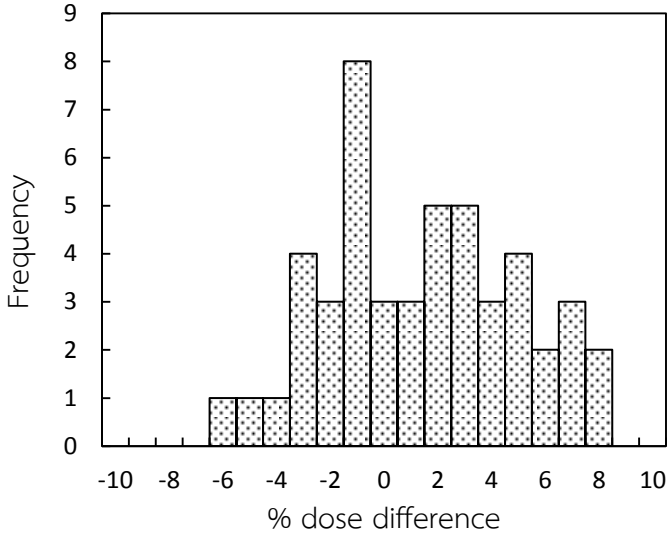

Figure 4.19 The distribution histogram of percentage dose difference between MuCheck and Eclipse for head and neck region in IMRT technique

4.2.2.3 Breast region in IMRT technique

The 42 cases of IMRT breast region were investigated; the mean of dose difference of MuCheck from Eclipse was -1.12 ± 2.30%. The discrepancy of MuCheck from Eclipse is shown in Figure 4.20 and its distribution that is presented in Figure 4.21 indicates the range of the discrepancy from -7.29% to 4.23%

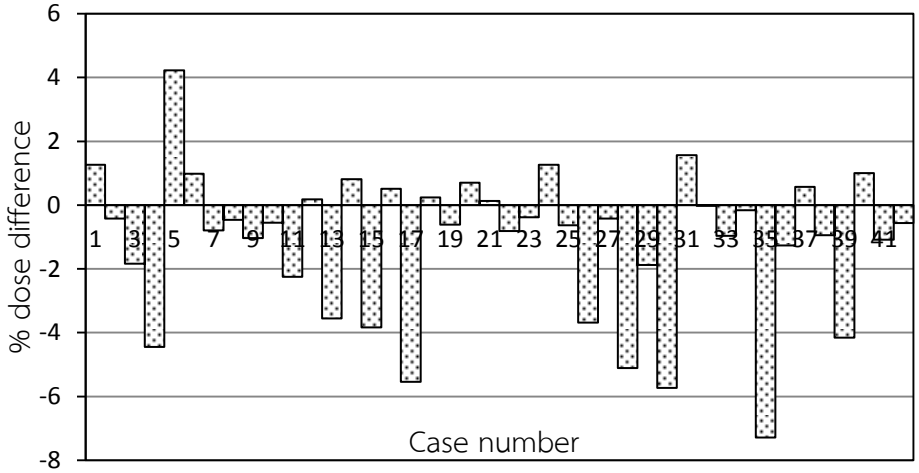

Figure 4.20 The dose difference between MuCheck and Eclipse for breast region in IMRT technique

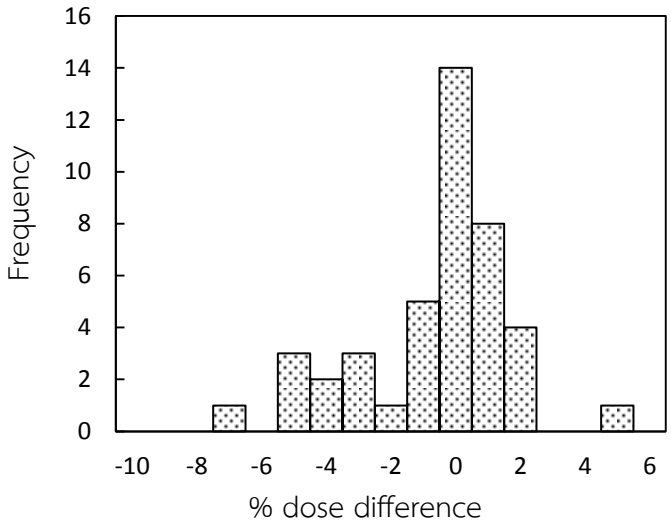

Figure 4.21 The distribution histogram of percentage dose difference between MuCheck and Eclipse for breast region in IMRT technique

4.2.2.4 Pelvis region in IMRT technique

The 41 cases of IMRT pelvis region were investigated; the mean of dose difference of MuCheck from Eclipse was 1.35 $\pm$ 2.74%. The discrepancy of MuCheck from Eclipse is shown in Figure 4.22 and its distribution that is presented in Figure 4.23 indicates the range of the discrepancy from -2.73% 7.5%

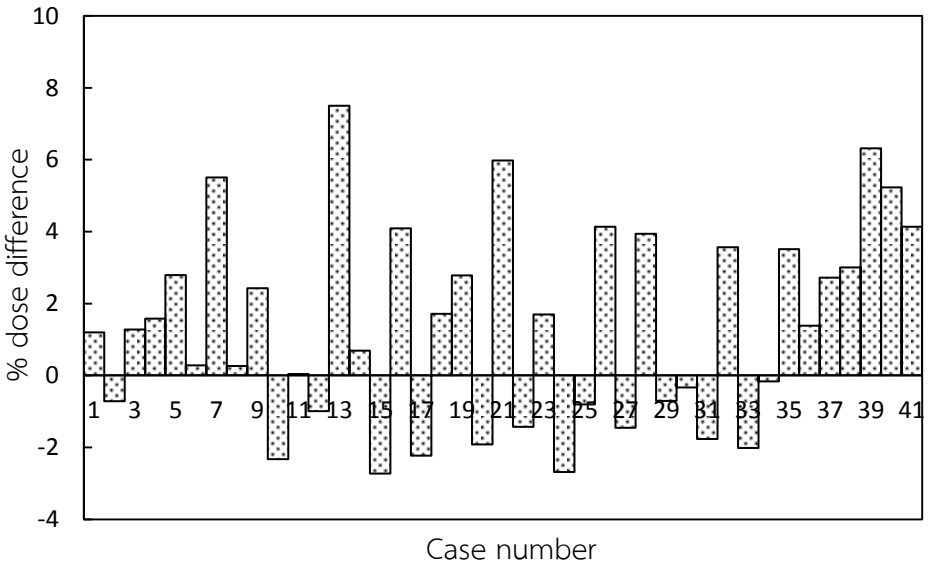

Figure 4.22 The dose difference between MuCheck and Eclipse for pelvis region in IMRT technique

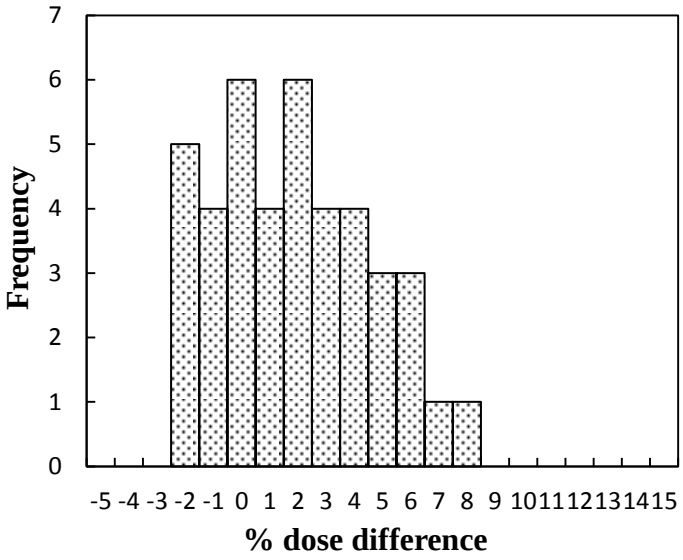

Figure 4.23 The distribution histogram of percentage dose difference between MuCheck and Eclipse for pelvis region in IMRT technique

4.2.2.5 All of treatment regions in IMRT technique

The 174 cases of IMRT plan for brain, head and neck, breast and pelvis were investigated; the mean of dose difference of MuCheck from Eclipse was 0.52±3.11%. The distribution of dose difference is presented in Figure 4.24.

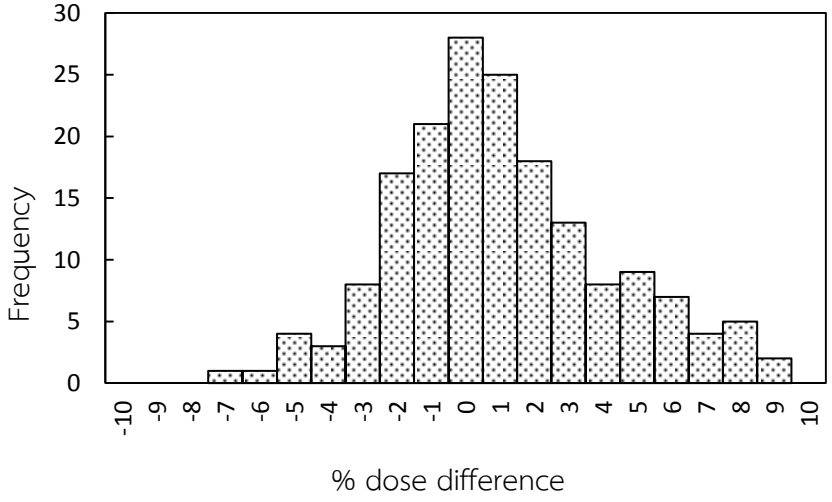

Figure 4.24 The distribution histogram of percentage dose difference between MuCheck and Eclipse in IMRT technique for all regions

CHAPTER V
DISCUSSION AND CONCLUSION

5.1 Discussion

Table 5.1 presents the verification of MuCheck for basic field sizes, that illustrates the difference of MuCheck from phantom measurement within the recommendation of IAEA TRS430(19) and AAPM TG 119(22).

Table 5.1 The confident limits of the difference between MuCheck and measurement

Field type	Confidence limit (%)
Open field	2.1
Wedged field	2.6
Composite field in 3D	1.3
Composite field in IMRT	4.8

The application of MuCheck compared to Eclipse TPS in clinical cases show 4.78% (1.5SD) limit of confidence for 3D technique and 5.18% (1.5SD) for IMRT technique that are acceptable. However, when the verification point is in the high dose gradient region, the dose difference is high in some cases. The confidence limits for individual treatment region in clinic are presented in Table 5.2 and Table 5.3. The difference could be higher than 5% for those cases and can be accepted at 7% such as *Xing et al.* (23) accepted higher than 7% or *Ting and Davis*'s reported(24) of acceptable value up to 10%.

Table 5.2 The dose difference between MuCheck and TPS applied in the clinical cases for 3D technique

Treatment region	Mean of difference (%)	SD (%)	Confidence limit (%)
Brain	2.57	1.16	4.31
Breast	1.85	2.87	6.15
Pelvis	1.44	0.84	2.70
All of 3 regions	1.98	1.87	4.78

Table 5.3 The dose difference between MuCheck and TPS applied in clinic for IMRT technique

Treatment region	Mean difference (%)	SD (%)	Confidence limit (%)
Brain	0.85	3.12	5.53
Head & neck	0.94	3.54	6.25
Breast	-1.12	2.30	4.57
Pelvis	1.35	2.74	5.46
All of 4 regions	0.52	3.11	5.18

Point dose verification method has its own limitation; the point doses are compared point to point without considering the distance-to-agreement or do not account for the dose gradient that add more or less systematic error to the comparison. Additionally, the difference of dose calculation algorithms deploy in MuCheck and Eclipse make the other systematic error. The analytical anisotropic algorithm (AAA) is used in Eclipse treatment planning system while conventional algorithm is employed in MuCheck. The AAA can correct for the inhomogeneity, irregular surface as well as the irregular field with block by acquiring the electron density from CT image. The beam in MuCheck is modeled in water and equivalent square field for block field is used, thus increasing the skin contouring effect and under estimate for collimator scatter factor and uncertainty in attenuation effect compared to the AAA calculation. So, in general, the dose calculated by MuCheck tends to be higher than calculated by Eclipse. Practically, the skin contouring and equivalent square field show large effect in 3D technique, which the fields cover the large area of irregular surface and shield the healthy organ by block. The skin contouring effect leads to large discrepancy of the data in breast area (as illustrated in Figure 5.1) with the SD equal to 2.87% compared to brain (SD = $\pm$1.16%) or pelvis (SD = $\pm$0.84%) areas in 3D technique, most of the cases of breast are treated by tangential fields. The equivalent square field for block field shows large effect in brain region, it makes the dose calculated by MuCheck much higher than Eclipse in 3D technique. The mean difference in brain is higher than breast and pelvis region because most of the brain cases are treated with block field but breast and pelvis are not.

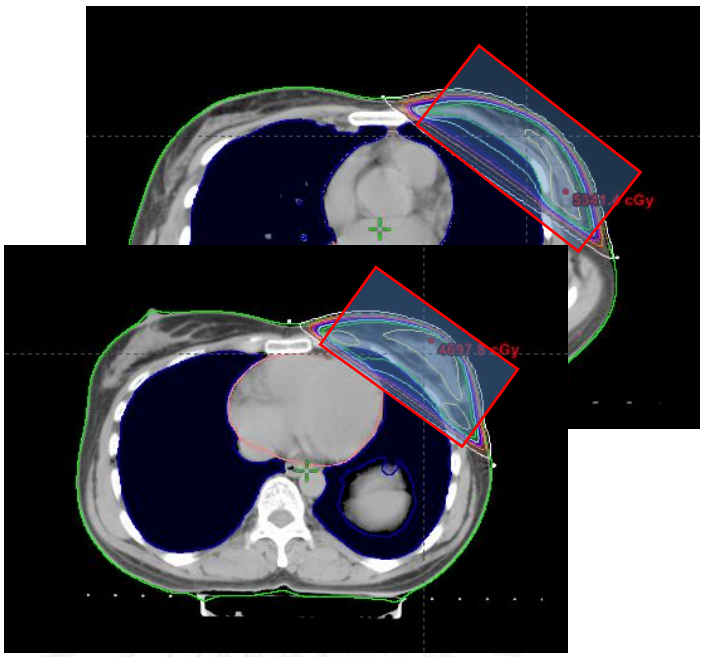

Figure 5.1 The various shapes of surface make enlarge the standard deviation of dose difference for breast region

The skin contouring effect and equivalent square field effect are not significant in IMRT technique but the effect of dose gradient is large, that make the data more scattered, large standard deviation for head & neck region compared to other regions.

5.2 Conclusion

The comparison of dose calculated by MuCheck and dose measured in water phantom was performed for open field, wedged field, composite field for 3D and IMRT. The confidence limits of dose difference are 2.1%, 2.6%, 1.3% and 4.8% for open field, wedged field, composite field in 3D and IMRT, respectively. The dose difference of MuCheck from phantom measurement is within the recommendation of IAEA TRS 430 and AAPM 119. So, MuCheck is accepted to apply in clinic with the real circumstance of treatment plan.

The application of MuCheck in clinical plans was investigated for 3D and IMRT techniques. For 3D technique, the confidence limits of dose difference from Eclipse are 4.30%, 6.16%, and 2.70% specified for brain, breast, and pelvis region, respectively. For all data of three treatment regions, the limitation of dose difference for 3D technique is 4.78%.

For IMRT technique, the confidence limit of dose difference from Eclipse are 5.53%, 6.25%, 4.57%, and 5.46% specified for brain, head and neck, breast and pelvis region, respectively. For all data of four treatment regions, the limitation of dose difference for IMRT technique is 5.18%.

The MuCheck independent dose calculation software can be employed as a verification tool in patient specific QA for all treatment regions in advanced treatment techniques.

According to the result of investigation, the application of MuCheck should be applied clinically for the treatment regions which less effect of the heterogeneity. The point dose should be compared point to point between MuCheck calculation and Eclipse calculation in the uniform dose volume. If the difference is greater than 5% for 3D or 5.2% for IMRT technique, the disparity should be resolved or apply the other approach of verification (e.g. measurement) before treatment.

REFERENCES

1. WHO. World Cancer factsheet. August 2012. Available from: http://publications.cancerresearchuk.org/downloads/product/CS_FS_WORLD_A4.pdf.
2. ICRU. Use of computers in external beam radiotherapy procedures with high-energy photons and electrons. ICRU. 1987;Report 42.
3. Stern RL, Heaton R, Fraser MW, Murty GS, Kirby TH, Lam KL, et al. Verification of monitor unit calculations for non-IMRT clinical radiotherapy: Report of AAPM Task Group 114. Med Phys. 2011;38(1):504-30.
4. Kutcher GJ, Coia L, Gillin M, Hanson WF, Leibel S, Morton RJ, et al. Comprehensive QA for radiation oncology: Report of AAPM Radiation Therapy Committee Task Group 40. Med Phys. 1994;21(4):581-618.
5. Dutreix A, Bjarngard BE, Bridier A, Mijnheer B, Shaw JE, Svensson H. Booklet 3 - Monitor Unit Calculation for High Energy Photon Beams. 1st edition. ESTRO. 1997.
6. Khan FM. The Physics of Radiation Therapy. 4th edition. Philadelphia,Lippincott Williams & Wilkins. 2010.
7. Sievinen J, Ulmer W, Kaissl W. AAA Photon Dose Calculation Model in Eclipse. Varian Medical System.
8. Khan FM. Treatment Planning in Radiation Oncology, 2nd Edition. Lippincott Williams & Wilkins. 2007.
9. ICRP. Prevention of accidental exposures to patients undergoing radiation therapy. ICRP. 2000;Publication 86.
10. Ravichandran R, Bhasi S, Binukumar JP, Davis CA. Need of patient-specific quality assurance and pre-treatment verification program for special plans in radiotheapy. Med Phys. 2011;36(3):181-3.
11. Alber M, Broggi S, Wagter CD, Eichwurzel I, Engström P, Fiorino C, et al. Guidelines for the verification of IMRT. First edition. ESTRO. 2008.
12. Karlsson M, Ahnesjö A, Georg D, Nyholm T, Olofsson J. Independent dose calculatIons concepts and models. First edition. ESTRO. 2010.
13. Haslam JJ, Bonta DV, Lujan AE, Rash C, Jackson W, Roeske JC. Comparison of dose calculated by an intensity modulated radiotherapy treatment planning system and an independent monitor unit verification program. Appl Clin Med Phys. 2003;4(3):224-30.
14. Chan J, Russell D, Peters VG, Farrell TJ. Comparison of monitor unit calculations performed with a 3D computerized planning system and independent "hand"

calculations: results of three years clinical experience. Appl Clin Med Phys. 2002;3(4):293-301.

15. Linthout N, Verellen D, Van Acker S, Storme G. A simple theoretical verification of monitor unit calculation for intensity modulated beams using dynamic mini-multileaf collimation. Radiother Oncol. 2004 May;71(2):235-41.
16. FDA certification for MuCheck program. Available from: http://www.accessdata.fda.gov/cdrh_docs/pdf/K980904.pdf.
17. IAEA. Absorbed Dose Determination in External Beam Radiotherapy. 2000;Technical reports series No. 98.
18. Fraass B, Doppke K, Hunt M, Kutcher G, Starkschall G, Stern R, et al. American Association of Physicists in Medicine Radiation Therapy Committee Task Group 53: Quality assurance for clinical radiotherapy treatment planning. Med Phys. 1998;25(10):1773-829.
19. IAEA. Commissioning and Quality Assurance of Computerized Planning Systems for Radiation Treatment of Cancer. 2004;Technical Reports Series No. 430.
20. Walker GA, Shostak J. Common Statistical Methods for Clinical Research with SAS® Examples. 2010;Third Edition.
21. Venselaar J, Welleweerd H, Mijnheer B. Tolerances for the accuracy of photon beam dose calculations of treatment planning systems. Radiother Oncol. 2001;60:191-201.
22. Ezzell GA, Burmeister JW, Dogan N, LoSasso TJ, Mechalakos JG, Mihailidis D, et al. IMRT commissioning: Multiple institution planning and dosimetry comparisons, a report from AAPM Task Group 119. Medical Physics. 2009;36(11):5359.
23. Xing L, Chen Y, Luxton G, Li JG, Boyer AL. Monitor unit calculation for an intensity modulated photon field by a simple scatter-summation algorithm. Phys Med Biol. 2000;45:N1-N7.
24. Ting JY, Davis LW. Dose verification for patients undergoing IMRT. Med Dosim. 2001;26:205-13.

APPENDICES

APPENDIX A

Table I. Data of dose difference between MuCheck and measurement for open field

No	MuCheck (cGy)	Measurement (cGy)	Diff (%)	No	MuCheck (cGy)	Measurement (cGy)	Diff (%)
1	85.86	87.44	-1.81	18	99.15	100.29	-1.13
2	91.79	92.28	-0.53	19	93.89	92.83	1.14
3	94.46	94.57	-0.12	20	93.85	94.24	-0.41
4	102.72	101.25	1.45	21	100.71	99.50	1.21
5	106.71	104.91	1.72	22	100.72	101.22	-0.49
6	92.60	91.40	1.31	23	96.89	98.37	-1.50
7	92.58	94.12	-1.64	24	101.98	101.98	0.00
8	86.00	87.10	-1.26	25	103.68	103.54	0.14
9	86.02	88.17	-2.44	26	110.56	107.87	2.49
10	94.48	94.02	0.49	27	113.95	110.46	3.16
11	94.43	95.20	-0.81	28	102.41	103.30	-0.86
12	93.71	93.52	0.20	29	102.40	101.12	1.27
13	98.65	98.24	0.42	30	96.95	98.42	-1.50
14	100.69	100.42	0.27	31	96.98	97.86	-0.90
15	106.58	106.16	0.40	32	103.70	103.86	-0.16
16	110.28	109.46	0.75	33	103.63	102.89	0.72
17	99.20	96.98	2.29				

Table II. Data of dose difference between MuCheck and measurement for wedged field

No	MuCheck (cGy)	Measurement (cGy)	Difference (%)
1	83.15	84.85	-2.01
2	87.64	87.73	-0.10
3	84.67	83.38	1.55
4	76.82	78.58	-2.24
5	73.02	73.03	-0.01
6	57.59	56.51	1.90
7	91.27	91.15	0.13
8	94.56	94.13	0.46
9	91.06	90.72	0.37
10	85.29	85.34	-0.06
11	80.97	80.61	0.45
12	65.63	65.09	0.83
13	94.53	95.84	-1.37
14	97.82	97.46	0.37
15	95.88	93.50	2.55
16	88.68	89.54	-0.96
17	84.90	83.94	1.14
18	70.47	68.06	3.55

Table III. Data of dose difference between MuCheck and measurement for composite field in 3D technique

No	MuCheck (cGy)	Measurement (cGy)	Difference (%)
1	440.13	443.01	-0.65
2	226.59	224.46	0.95
3	223.88	223.92	-0.02
4	247.51	246.48	0.42
5	399.29	397.55	0.44
6	215.92	215.33	0.27
7	350.17	347.56	0.75
8	293.65	291.56	0.72
9	240.86	240.40	0.19
10	215.06	212.58	1.16
11	194.93	196.46	-0.78
12	216.93	217.24	-0.14
13	232.92	235.90	-1.26
14	341.92	338.33	1.06
15	313.64	314.92	-0.41

Table IV. Data of dose difference between MuCheck and measurement for composite field in IMRT technique

No	MuCheck (cGy)	Measurement (cGy)	Diff (%)	No	MuCheck (cGy)	Measurement (cGy)	Diff (%)
1	214.99	214.40	0.27	21	285.24	293.14	-2.69
2	134.77	134.32	0.34	22	212.36	218.61	-2.86
3	113.97	119.32	-4.48	23	186.24	189.40	-3.50
4	239.30	244.91	-2.29	24	1482.55	1412.30	3.53
5	294.95	302.13	-2.38	25	213.44	219.88	-2.00
6	266.38	271.65	-1.94	26	209.06	210.70	-2.31
7	268.41	258.36	3.89	27	231.54	233.69	-2.01
8	281.57	272.17	3.45	28	250.19	245.73	1.33
9	271.07	258.66	4.80	29	237.55	238.53	-1.06
10	255.23	257.26	-0.79	30	229.06	235.28	-3.43
11	212.73	210.77	0.93	31	205.98	205.61	-2.94
12	194.68	204.03	-4.58	32	228.36	231.23	-0.89
13	196.18	203.05	-3.39	33	206.02	208.95	-2.13
14	203.02	214.80	-5.48	34	226.17	215.99	2.66
15	265.57	274.35	-3.20	35	221.19	224.46	-2.34
16	205.62	209.85	-2.02	36	230.55	227.92	0.90
17	272.67	278.32	-2.03	37	535.34	516.96	5.65
18	208.32	210.51	-1.04	38	235.57	227.73	2.60
19	274.12	281.23	-2.53	39	213.71	217.71	-2.81
20	202.11	206.94	-2.34				

APPENDIX B

Table V. The percentage dose difference between MuCheck and Eclipse in clinical application in 3D technique for brain region

No.	MuCheck (cGy)	Eclipse (cGy)	Diff (%)	No.	MuCheck (cGy)	Eclipse (cGy)	Diff (%)
1	209.54	206.18	1.60	24	189.95	187.41	1.33
2	204.02	200.00	1.97	25	258.70	250.00	3.36
3	221.59	220.00	0.72	26	308.73	300.00	2.83
4	209.31	204.08	2.50	27	205.22	200.00	2.54
5	309.48	300.00	3.06	28	217.28	210.53	3.11
6	318.92	309.28	3.02	29	321.50	315.23	1.95
7	227.80	225.00	1.23	30	188.90	180.00	4.71
8	258.15	250.00	3.16	31	194.55	189.48	2.61
9	215.22	210.53	2.18	32	192.60	188.66	2.05
10	204.66	200.00	2.28	33	214.74	209.83	2.28
11	190.64	185.57	2.66	34	218.71	209.00	4.44
12	195.55	189.48	3.11	35	309.43	300.00	3.05
13	304.47	306.12	-0.54	36	196.78	189.48	3.71
14	194.76	189.47	2.72	37	211.67	211.51	0.08
15	310.53	300.00	3.39	38	306.99	304.18	0.92
16	308.75	300.00	2.83	39	208.97	202.45	3.12
17	310.95	300.00	3.52	40	314.48	305.29	2.92
18	328.74	315.79	3.94	41	217.86	212.71	2.36
19	205.05	200.00	2.46	42	192.92	187.50	2.81
20	188.61	180.00	4.56	43	186.80	183.78	1.62
21	214.50	208.33	2.87	44	316.93	312.50	1.40
22	194.16	185.57	4.42	45	219.40	211.36	3.66
23	192.88	186.42	3.35	46	185.68	185.10	0.31

Table VI. The percentage dose difference between MuCheck and Eclipse in clinical application in 3D technique for breast region

No.	MuCheck (cGy)	Eclipse (cGy)	Diff (%)	No.	MuCheck (cGy)	Eclipse (cGy)	Diff (%)
1	211.59	218.92	-3.47	21	208.88	200.00	4.25
2	218.90	213.57	2.43	22	208.92	200.00	4.27
3	201.38	200.00	0.69	23	216.48	210.44	2.79
4	319.60	307.68	3.73	24	214.90	210.53	2.03
5	209.36	204.91	2.12	25	214.11	204.08	4.68
6	313.75	300.00	4.38	26	217.56	210.53	3.23
7	221.10	210.53	4.78	27	296.99	308.14	-3.75
8	294.20	284.21	3.39	28	185.34	196.71	-6.14
9	212.09	206.18	2.78	29	196.80	200.00	-1.63
10	211.28	205.91	2.54	30	198.74	200.00	-0.63
11	215.72	206.19	4.42	31	232.56	236.74	-1.80
12	288.14	284.21	1.36	32	277.10	273.58	1.27
13	212.28	206.19	2.87	33	199.24	200.00	-0.38
14	191.92	199.87	-4.14	34	210.53	200.00	5.00
15	283.58	272.13	4.04	35	201.42	200.00	0.70
16	217.69	207.96	4.47	36	202.37	200.00	1.17
17	288.96	278.35	3.67	37	206.65	200.00	3.22
18	219.63	224.51	-2.22	38	206.20	200.00	3.01
19	283.59	271.46	4.28	39	206.26	204.08	1.06
20	217.86	206.52	5.21	40	209.38	200.00	4.48

Table VII. The percentage dose difference between MuCheck and Eclipse in clinical application in 3D technique for pelvis region

No.	MuCheck (cGy)	Eclipse (cGy)	Diff (%)	No.	MuCheck (cGy)	Eclipse (cGy)	Diff (%)
1	188.76	183.67	2.70	22	193.31	189.47	1.99
2	183.93	183.70	0.13	23	209.68	206.21	1.66
3	201.89	200.00	0.94	24	229.5	225.00	1.96
4	193.82	189.47	2.24	25	310.37	309.31	0.34
5	183.82	180.03	2.06	26	201.53	200.01	0.76
6	195.29	189.47	2.98	27	200.7	199.85	0.42
7	301.18	299.97	0.40	28	207.34	204.05	1.59
8	182.15	180.00	1.18	29	188.72	185.57	1.67
9	186.5	183.66	1.52	30	207.82	206.24	0.76
10	184.02	179.96	2.21	31	188.39	185.53	1.52
11	210.56	206.15	2.10	32	206.6	204.08	1.22
12	313.33	306.13	2.30	33	304.65	300.00	1.53
13	208.58	206.16	1.16	34	189.31	187.50	0.96
14	188.39	185.48	1.54	35	213.55	210.54	1.41
15	188.96	185.59	1.78	36	209.14	206.18	1.41
16	319.41	309.31	3.16	37	203.04	200.05	1.47
17	205.51	208.33	-1.37	38	193.04	189.50	1.83
18	194.13	189.44	2.42	39	315.88	309.41	2.05
19	213.7	210.52	1.49	40	191.26	189.47	0.93
20	187.75	185.51	1.19	41	186.08	185.50	0.31

APPENDIX C

Table VIII. The percentage dose difference between MuCheck and Eclipse in clinical application in IMRT technique for brain region

No.	MuCheck (cGy)	Eclipse (cGy)	Diff (%)	No.	MuCheck (cGy)	Eclipse (cGy)	Diff (%)
1	181.26	184.90	-2.01	23	328.01	325.71	0.70
2	1425.01	1323.70	7.11	24	238.43	218.55	8.34
3	204.2	208.40	-2.06	25	1390.32	1320.00	5.06
4	195.88	199.96	-2.08	26	209.52	209.61	-0.05
5	208.37	208.66	-0.14	27	228.16	208.54	8.60
6	211.48	200.21	5.33	28	311.67	309.25	0.78
7	303.11	300.05	1.01	29	197.33	202.82	-2.78
8	187.05	184.79	1.21	30	220.95	223.17	-1.00
9	190.29	189.83	0.24	31	208.06	202.19	2.82
10	185.36	186.84	-0.80	32	206.76	202.05	2.28
11	201.28	204.54	-1.62	33	184.01	185.17	-0.63
12	216.54	210.53	2.77	34	1756.86	1683.80	4.16
13	202.19	204.31	-1.05	35	123.88	119.56	3.49
14	193.75	199.30	-2.86	36	306.68	315.14	-2.76
15	182.42	180.66	0.97	37	206.76	210.27	-1.70
16	201.05	200.60	0.22	38	213.08	211.28	0.85
17	205.22	210.48	-2.56	39	183.36	181.28	1.13
18	197.98	198.89	-0.46	40	232.95	232.93	0.01
19	197.46	204.25	-3.44	41	203.04	202.96	0.04
20	202.18	207.28	-2.52	42	205.98	205.61	0.18
21	211.39	211.16	0.11	43	210.21	206.00	2.00
22	566.71	522.48	7.80				

Table IX. The percentage dose difference between MuCheck and Eclipse in clinical application in IMRT technique for head and neck region

No.	MuCheck (cGy)	Eclipse (cGy)	Diff (%)	No.	MuCheck (cGy)	Eclipse (cGy)	Diff (%)
1	193.78	186.62	3.70	25	220.33	217.19	1.42
2	125.60	122.76	2.26	26	239.62	243.20	-1.49
3	230.29	223.66	2.88	27	128.20	123.01	4.05
4	242.28	229.84	5.13	28	223.66	229.45	-2.59
5	238.16	232.46	2.39	29	201.84	201.14	0.35
6	211.24	214.25	-1.42	30	123.86	125.28	-1.15
7	227.41	235.83	-3.70	31	120.58	124.85	-3.54
8	236.34	240.27	-1.66	32	213.80	205.74	3.77
9	109.35	108.41	0.86	33	192.17	193.55	-0.72
10	192.74	180.48	6.36	34	230.96	238.00	-3.05
11	188.43	190.17	-0.92	35	300.75	320.03	-6.41
12	206.17	202.88	1.59	36	197.92	190.84	3.58
13	238.35	248.80	-4.38	37	230.01	225.46	1.98
14	230.01	214.79	6.62	38	197.86	208.30	-5.28
15	303.86	311.67	-2.57	39	205.08	208.59	-1.71
16	162.89	151.05	7.27	40	216.09	211.99	1.90
17	236.34	240.27	-1.66	41	206.67	191.27	7.45
18	204.33	203.00	0.65	42	219.87	214.52	2.43
19	199.33	199.41	-0.04	43	228.40	218.52	4.32
20	244.61	230.22	5.88	44	189.55	195.01	-2.88
21	231.50	227.69	1.64	45	179.37	181.46	-1.16
22	200.33	203.90	-1.78	46	192.90	183.62	4.81
23	98.32	94.23	4.16	47	190.58	178.41	6.38
24	218.07	213.14	2.26	48	133.38	137.44	-3.04

Table X. The percentage dose difference between MuCheck and Eclipse in clinical application in IMRT technique for breast region

No.	MuCheck (cGy)	Eclipse (cGy)	Difference %	No.	MuCheck (cGy)	Eclipse (cGy)	Difference %
1	202.55	200.00	1.26	22	267.82	270.00	-0.81
2	272.70	273.84	-0.42	23	205.39	206.19	-0.39
3	201.28	204.99	-1.84	24	208.81	206.18	1.26
4	179.17	187.14	-4.45	25	188.27	189.47	-0.64
5	208.83	200.00	4.23	26	197.07	204.34	-3.69
6	201.99	200.00	0.99	27	273.06	274.23	-0.43
7	184.10	185.57	-0.80	28	200.29	210.53	-5.11
8	205.24	206.18	-0.46	29	202.39	206.18	-1.87
9	204.06	206.18	-1.04	30	195.00	206.18	-5.74
10	205.05	206.19	-0.55	31	263.73	259.61	1.56
11	201.95	206.49	-2.25	32	200.88	200.92	-0.02
12	210.90	210.53	0.18	33	198.08	200.00	-0.97
13	201.17	208.33	-3.56	34	203.74	204.08	-0.17
14	276.46	274.23	0.81	35	196.22	210.53	-7.29
15	257.13	267.00	-3.84	36	207.89	210.53	-1.27
16	201.02	200.00	0.51	37	166.30	165.36	0.57
17	252.98	267.00	-5.54	38	208.56	210.53	-0.94
18	200.47	200.00	0.23	39	195.94	204.08	-4.15
19	265.37	267.00	-0.61	40	206.15	204.08	1.00
20	212.01	210.53	0.70	41	197.86	200.00	-1.08
21	267.34	267.00	0.13	42	198.88	200.00	-0.56

Table XI. The percentage dose difference between MuCheck and Eclipse in clinical application in IMRT technique for pelvis region

No.	MuCheck (cGy)	Eclipse (cGy)	Difference %	No.	MuCheck (cGy)	Eclipse (cGy)	Difference %
1	229.80	227.06	1.19	22	168.97	171.38	-1.43
2	209.27	210.78	-0.72	23	211.19	207.62	1.69
3	204.13	201.53	1.27	24	201.54	206.95	-2.68
4	258.29	254.20	1.58	25	202.94	204.58	-0.81
5	209.27	203.42	2.79	26	160.82	154.16	4.14
6	207.20	206.62	0.28	27	202.40	205.35	-1.46
7	219.98	207.86	5.51	28	236.78	227.46	3.94
8	200.45	199.92	0.26	29	209.14	210.63	-0.71
9	206.40	201.40	2.42	30	188.80	189.43	-0.33
10	198.58	203.20	-2.33	31	201.74	205.31	-1.77
11	205.88	205.80	0.04	32	212.80	205.21	3.57
12	206.26	208.31	-0.99	33	108.27	110.45	-2.02
13	252.36	233.43	7.50	34	222.75	223.11	-0.16
14	209.21	207.76	0.69	35	199.16	192.17	3.51
15	91.07	93.56	-2.73	36	193.09	190.42	1.38
16	234.54	224.94	4.09	37	199.63	194.20	2.72
17	168.61	172.37	-2.23	38	210.79	204.46	3.00
18	160.26	157.52	1.71	39	244.90	229.43	6.32
19	198.95	193.42	2.78	40	221.71	210.12	5.23
20	204.76	208.69	-1.92	41	208.53	199.91	4.13
21	224.16	210.76	5.98				

VITA

Name:	Vinh Cao Huu
Date of Birth:	October 05, 1986
Place of Birth:	Binh Thuan, Vietnam
Email address:	caohuuvinh@gmail.com
Institutions Attended:	
	- Bachelor of Science, University of Natural Sciences – National University of Ho Chi Minh City, 2008
	- Nuclear Energy training, Vietnam Atomic Energy Agency, 2009
	- Master of Science, Chulalongkorn University, Bangkok, Thailand, 2013
Permanent Address:	17 Hamlet Minh Hoa, Ham Minh Ward, Ham Thuan Nam District, Binh Thuan Province, Vietnam